THE REACTIONS OF TRIDEUTEROMETHYL RADICALS WITH TETRAMETHYLGERMANE AND TETRAMETHYLSTANNANE

by

Peter William Slade

B.Sc., University of Southampton, 1968

A THESIS SUBMITTED IN PARTIAL FULFILMENT OF

THE REQUIREMENTS FOR THE DEGREE OF

MASTER OF SCIENCE

in the Department

of

Chemistry

SIMON FRASER UNIVERSITY

April 1971

APPROVAL

Name: Peter William Slade

Degree: Master of Science

Title of Thesis: The Reactions of Trideuteromethyl Radicals with Tetramethylgermane and Tetramethylstannane

Examining Committee:

Chairman: Dr. D. Sutton

Dr. T. N. Bell
Senior Supervisor

Dr. L. K. Peterson

Dr. A. G. Sherwood

Dr. A. C. Oehlschlager

Date Approved: May 27, 1971

Abstract

This thesis describes the reactions resulting from the interactions of free radicals with substrates containing a group IV element as the central atom. Previous work has been surveyed and the author's own work described. The latter consists of the measurement of the Arrhenius parameters for the abstraction of hydrogen from tetramethylgermane and tetramethylstannane with trideuteromethyl radicals. Radical exchange in these systems has also been studied.

This completes the data on the reactions of both trifluoromethyl and trideuteromethyl radicals with the group IV tetramethyls.

Dedication

to

Sheila Ann

my sister Brenda

and my mother

Acknowledgement

I wish to thank Dr. T. N. Bell for his supervision of my research and for his most helpful criticism during the preparation of this thesis.

I should also like to thank my other committee members, Dr. L. K. Peterson and Dr. A. G. Sherwood, for their help and friendly discussions; and Post-Doctoral Research Fellows, Dr. R. E. Berkley and Dr. A. E. Platt, for their guidance in the laboratory.

I am indebted to the National Research Council for financial assistance and to Miss Sheila Ann Dodge for typing this thesis.

Contents

Contents Continued

Contents Continued

List of Graphs

The Reactions of Trideuteromethyl Radicals

with

Tetramethylgermane

and

Tetramethylstannane

1. Introduction.

Considerable work has been carried out on the reactions of free radicals with organic compounds but until recently, little had been attempted with inorganic substrates. Studies of the latter are of interest with respect to the relationship of their reactivity to the general properties of the central metal atom. For instance, the properties of a molecule may be altered distinctly if carbon is replaced by other group IV elements. Consider the following data[1]:

		Electronegativity (a)	Electronegativity (b)	Covalent Radius (Å)
C	$[He]\ 2s^2\ 2p^2$	2.55	2.50	0.77
Si	$[Ne]\ 3s^2\ 3p^2$	1.90	1.74	1.17
Ge	$[Ar]\ 3d^{10}\ 4s^2\ 4p^2$	2.01	2.02	1.22
Sn	$[Kr]\ 4d^{10}\ 5s^2\ 5p^2$	1.96	1.72	1.40 *
Pb	$[Xe]\ 4f^{14}\ 5d^{10}\ 6s^2\ 6p^2$	2.33	1.55	1.54‡

(a) = Pauling series : C > Pb > Ge > Sn > Si
(b) = Allred and Rochow series : C > Ge > Si ~ Sn > Pb

* = covalent radius of Sn^{II}

‡ = ionic radius of Pb^{II}

The group IV elements provide a striking example of an enormous discontinuity in general properties between the first and second members, carbon and silicon respectively, followed by a fairly smooth change toward more metallic character in the elements after silicon. The electronegativities do not increase monatonically, which has been rationalized in terms of the filling of the d, and later, f orbitals in the transition elements and lanthanides respectively, which affects the nuclear screening of the elements following.

In general, the hydrides of the remaining group IV elements, and their derivatives, are considerably more reactive than the carbon analogues in hydrogen abstraction reactions.

The silanes have been investigated, (see reference 2 and appendix 1), and found to show higher reactivity for hydrogen abstraction compared with the analogous carbon compounds. This can be related to the respective bond strengths; the

covalent bond strength of Si-H is about 25 kcal. mole^{-1} lower than that of C-H.

The Ge-H and Sn-H covalent bond strengths are similar to that of Si-H[1],

M =	C	Si	Ge	Sn
M-H bond strength (kcal. mole^{-1})	99	75	74	71

Similar higher reactivity is noted for hydrogen abstraction in substituted silanes, (for instance those containing methyl groups and halogen atoms), compared with the carbon analogues. This can be attributed to the difference in electronegativities and to the utilization by silicon of its d orbitals. The latter aspect can manifest itself in two ways: silicon can increase its co-ordination number to five or six; π-bonding may occur between the empty silicon d orbitals and suitably filled ligand orbitals of the correct symmetry and spatial orientation[3,4].

A similar influence of d orbitals is also expected with germanium and tin systems.

Recent studies have included those of free radicals, mainly $\cdot CH_3$, $\cdot CD_3$ and $\cdot CF_3$, with inorganic substrates, in particular the halosilanes[5,6,7], methylhalosilanes[8,9,10,11], and the group IV tetramethyls[12,13,14,15].

The results of hydrogen abstraction from the methylfluorosilanes, $(CH_3)_{4-X}SiF_X$ where x = 0 - 3, using $\cdot CD_3$[9], and $\cdot CF_3$[8], radicals demonstrate the differences between the reactivities of the radicals.

A graph of activation energy for abstraction plotted against proton chemical shift shows a gentle curve, increasing from $(CH_3)_4Si$ to CH_3SiF_3 for both $\cdot CD_3$ and $\cdot CF_3$ radical attack. Since the F_3C-H bond is some 2kcal. mole^{-1} higher in energy than D_3C-H, one might expect parallel curves, separated by a function of the difference in bond energies.

In fact, the difference between the activation energies increases from CH_3SiF_3 to $(CH_3)_4Si$ and this is rationalized by considering the influence of both the inductive effect of

the F atom(s) on the C-H bond strength, and the polar effect which can be repulsive or attractive depending on the interaction of the electrophilic $\cdot CF_3$ radical with protonic or hydridic hydrogen atoms, respectively.

The same graph for hydrogen abstraction from the corresponding methylchlorosilanes by $\cdot CF_3$ radicals[10], produces a different curve. After an initial rise of about 2kcal. $mole^{-1}$ from $(CH_3)_4Si$ to $(CH_3)_3SiCl$, little difference in activation energy is noted between the latter, $(CH_3)_2SiCl_2$ and CH_3SiCl_3. To account for this similarity it is suggested that $p\pi$-$d\pi$ Cl-Si back bonding occurs from filled Cl p orbitals to the empty Si d orbitals, which renders the polar effect constant.

In the last year or so, work has been reported on the abstraction of hydrogen from all the group IV tetramethyls using $\cdot CH_3$[13,14], CD_3[15], and $\cdot CF_3$[12,14,16] radicals. In particular, Arrhenius parameters were measured for hydrogen abstraction from $C(CH_3)_4$, $Si(CH_3)_4$, $Ge(CH_3)_4$ and $Sn(CH_3)_4$ using $\cdot CF_3$ radicals[12]. A plot of log k for abstraction against chemical shift shows a gentle curve where log k decreases in the order Si > Sn > Ge > C which is the order of increasing electronegativity of the group IV element.

After losing a hydrogen atom by abstraction, the tetramethyl substrate may combine with a $\cdot CF_3$ radical to produce a hot molecule[8,17] which can either be stabilized by collision, or can undergo a β-fluoro rearrangement with subsequent elimination of an olefin:

$$\cdot CF_3 + \cdot CH_2M(CH_3)_3 \longrightarrow CH_3CH_2M(CH_3)_3^{*} \xrightarrow{N} CF_3CH_2M(CH_3)_3$$
$$\searrow CF_2CH_2 + FM(CH_3)_3$$

where M = Si, Ge or Sn. N = third body.

The stabilized molecule may also produce an olefin by thermolysis:

$$CF_3CH_2M(CH_3)_3 \xrightarrow{\Delta} CF_2CH_2 + FM(CH_3)_3$$

Also, evidence has been found for radical exchange, (exchange between attacking $\cdot CF_3$ radicals and substrate CH_3

groups[18]):

$$\cdot CF_3 + M(CH_3)_4 \rightleftarrows [CF_3 - M(CH_3)_4] \rightarrow [CF_3M(CH_3)_3] + \cdot CH_3$$

It has been noted that the hot molecule rearrangement-elimination reaction occurs when the central metal atom has empty d orbitals available for bonding and that the radical exchange mechanism, which requires a five co-ordinate intermediate, is observed for Si, Ge and Sn, that is, where the central (group IV) atom can utilize its d orbitals to attain a co-ordination number greater than four. Investigation of the reaction of $\cdot CF_3$ and $\cdot CD_3$ radicals with $B(CH_3)_3$, trimethylborane,[30] has also yielded evidence for similar exchange and elimination reactions. In this case it is assumed that the empty p orbital is used.

These aspects are considered of sufficient interest to warrant further work in connexion with this field.

2. Review of Previous Work.

2.1. Hydrogen Abstraction Reactions from Methylhalosilanes using $\cdot CD_3$ and $\cdot CF_3$ radicals; references 8, 9, 10, 11.

The Arrhenius parameters have been measured for this process in the case of the series $(CH_3)_4Si$, $(CH_3)_3SiX$, $(CH_3)_2SiX_2$, CH_3SiX_3 where X = F or Cl.

The work was performed with $\cdot CF_3$ and $\cdot CD_3$ radicals for the methylfluorosilanes and with $\cdot CF_3$ radicals in the case of the methylchlorosilanes. Hexafluoroacetone (HFA) and hexadeuteroacetone (HDA) were photolyzed to produce, respectively, $\cdot CF_3$ and $\cdot CD_3$ radicals.

The HFA + methylfluorosilane system was extensively investigated to check the possibility that the products of radical reactions were produced from a reaction of excited HFA molecules and the substrate. A study of the emission spectrum of HFA showed that the silanes only slightly enhanced the spectra (an effect similar to that of CO_2) and quenching was noted when oxygen was used. The volatile products of the photolysis of HFA mixed with silane were CO, C_2F_6, CF_3H and CF_2CH_2, the latter three being reduced by addition of oxygen and wholly suppressed by 16 torr of the same gas; that is, oxygen acts as a radical scavenger.

The same products were obtained if hexafluoroazomethane (HFAM) was used as a radical source and since methane products were not detected from the photolysis of HFA or HFAM alone, they must come from the HFA + silane system. (Methane is also produced by abstraction of hydrogen from unphotolyzed HDA by $\cdot CD_3$ radicals.)

2.1.1. Results.

The results obtained for work done on these systems are as follows:

	$\cdot CD_3$		$\cdot CF_3$	
	Log A	E_A (kcal mole^{-1})	Log A	E_A (kcal mole^{-1})
$(CH_3)_4Si$	12.0±0.10	10.79±0.22	11.91±0.09	7.29±0.14
$(CH_3)_3SiF$	12.0±0.12	11.53±0.21	12.43±0.05	9.48±0.09
$(CH_3)_2SiF_2$	12.0±0.05	12.11±0.12	12.27±0.06	10.53±0.12
CH_3SiF_3	12.1±0.12	12.56±0.25	11.98±0.04	11.71±0.09
$(CH_3)_3SiCl$			12.25±0.06	9.13±0.09
$(CH_3)_2SiCl_2$			11.79±0.09	9.23±0.18
CH_3SiCl_3			11.31±0.13	9.35±0.21

2.1.2. Interpretation of Results

The values obtained by Kerr[5] for the HDA + methylchlorosilanes showed A factors outside the normal range of 11.5 - 12.5 and were doubted on this ground by other workers. Kerr re-investigated some other systems which had also shown abnormal A factors[7,16] and found the subsequent values to be in the normal range. Although the HDA + methylchlorosilane systems were not re-investigated, Kerr's values are considered suspect and are not included.

Considering the HDA + methylfluorosilane system, a plot of activation energy v. proton chemical shift indicates that the reactivity of the silanes is decreased as F atoms replace CH_3 groups. This can be explained in terms of the inductive effect of the F atom(s) which reduces the electron density on the H atom undergoing abstraction, (H_a).

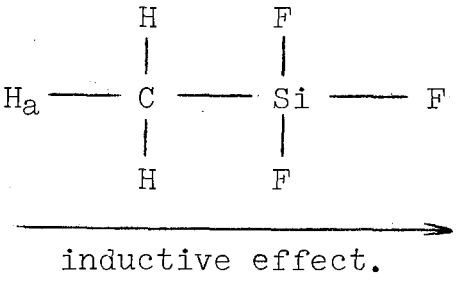

The removal of electron density from H_a strengthens the $C-H_a$ bond, making the abstraction of the H_a less facile. The $C-H_a$ bond strength is thus a function of F-substitution as indicated by the bond strength data obtained from the Polanyi equation which has been tested by Trotman-Dickenson[22]:

$$E = 0.49\ (D_{C-H} - 74.3)$$

	D_{C-H} kcal. mole^{-1}	
$(CH_3)_4Si$	96.3	97.0
$(CH_3)_3SiF$	97.8	
$(CH_3)_2SiF_2$	99.0	
CH_3SiF_3	99.9	
	(9)	(16)

For the HFA + methylfluorosilane systems a plot of activation energy v. proton chemical shift produces a curve below the $\cdot CD_3$ curve; the differences for each silane increases as F atoms are replaced by CH_3 groups.

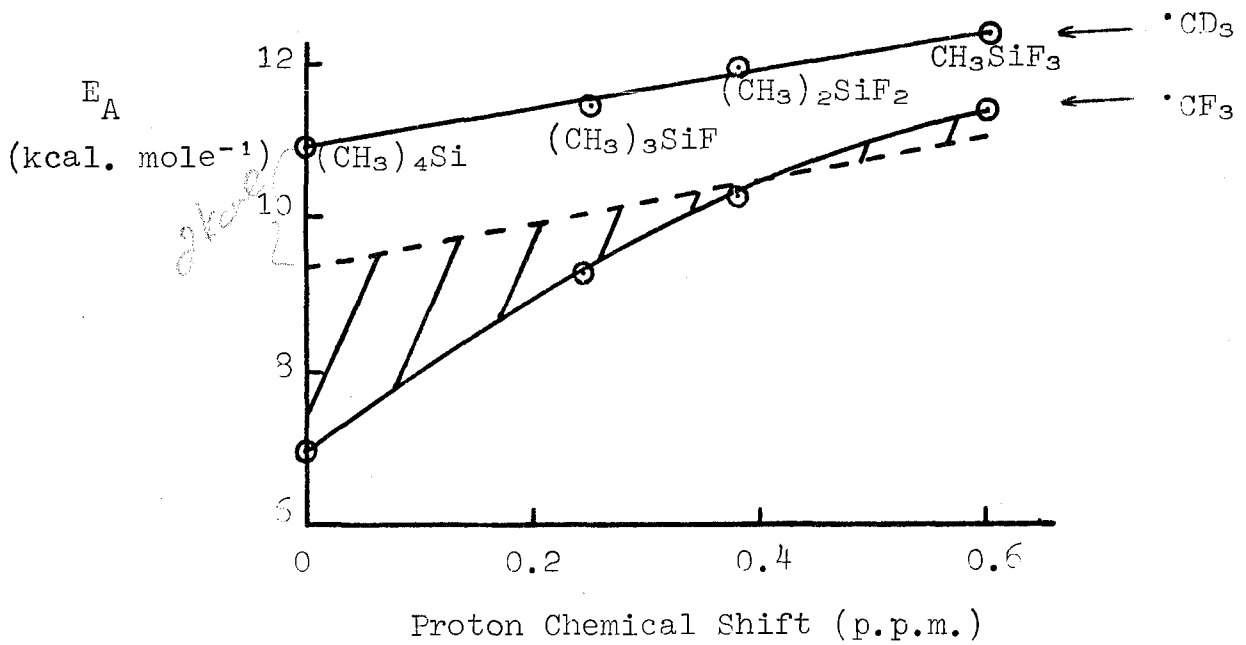

A difference in activation energy for hydrogen abstraction from a particular silane with the different radicals is expected because of the added inductive effect of the F atoms present in the $\cdot CF_3$ radical. This is referred to as the polar effect.

One can predict the difference expected on heats of reaction differences for a given silane based on the bond energy differences,

$$(D_{F_3C-H} - D_{H_3C-H} \approx 106 - 104 \approx 2 \text{kcal. mole}^{-1})$$

Consider the relationship between the bond energies and activation energies for hydrogen abstraction from $C(CH_3)_4$ and $Si(CH_3)_4$ using $\cdot CD_3$ radicals:

D_{C-H} for $C(CH_3)_4$	D_{C-H} for $Si(CH_3)_4$	$E_{C(CH_3)_4} - E_{Si(CH_3)_4}$
(kcal. mole^{-1})	(kcal. mole^{-1})	(kcal. mole^{-1})
~ 99	~ 97	12.0 - 10.8 = 1.2 (reference 12)
		12.0 - 10.4 = 1.6 (reference 16)

Thus for a difference in bond energies of about 2kcal. mole^{-1}, a difference in activation energies of about 1.5kcal. mole^{-1} is observed. Since the difference $D_{F_3C-H} - D_{H_3C-H}$ is also about 2kcal. mole^{-1}, a difference in activation energies for hydrogen abstraction by $\cdot CF_3$ and $\cdot CD_3$ radicals of 1.5kcal. mole^{-1} might be expected for each silane.

Such a constant difference is not observed, indicating that additional factors have some influence.

	$E_{CD_3} - E_{CF_3}$ (kcal. mole^{-1})
$(CH_3)_4Si$	3.5
$(CH_3)_3SiF$	2.1
$(CH_3)_2SiF_2$	1.6
CH_3SiF_3	0.8

The variation of this difference for each silane to that expected from the aspect of bond energies, (1.5kcal. mole^{-1}), is attributed to the polar effect.

The polar effect arises from the interaction of the

electrophilic $\cdot CF_3$ radical with methyl hydrogens. If the methyl hydrogens are hydridic, as in the case of $(CH_3)_4Si$, then the attractive polar effect is enhanced and the activation energy for hydrogen abstraction by $\cdot CF_3$ radicals is lower than that anticipated by bond dissociation energy considerations; thus the difference $E_{CD_3} - E_{CF_3}$ is higher.

However, as the methyl groups are replaced by fluorine atoms, the hydrogen atoms of the remaining methyl groups become more protonic. In the case of CH_3SiF_3 the methyl hydrogens are protonic in nature and it is the repulsive polar effect that is enhanced. Thus the activation energy for the same process is higher than anticipated solely from bond dissociation energy considerations and the difference $E_{CD_3} - E_{CF_3}$ is lower.

The bond dissociation energy argument is, perhaps, only semi-quantitative, but it is sufficient to demonstrate the deviation from parallelism of the curves.

If one considers the $\cdot CF_3$ radical to be electrophilic, then the polar effect operating to lower the activation energy for $(CH_3)_4Si$, (and $(CH_3)_3SiF$), can be introduced into a Polanyi type equation:

$$E_A \propto (\text{constant} - \Delta H) - \delta_{\substack{\text{polar} \\ \text{effect.}}}$$

The fact that ΔE_A is lower than that anticipated on ΔH considerations can be explained in terms of Ha becoming more protonic in nature. For the case of compounds with protonic hydrogens, $E_{A(CF_3)} > E_{A(CD_3)}$. For example: HCl, HBr, H_2S and $HSiCl_3$.

A similar plot for the HFA + methylchlorosilanes shows that after a 2kcal. $mole^{-1}$ rise in activation energy from $(CH_3)_4Si$ to $(CH_3)_3SiCl$ there is a mere 200cal. $mole^{-1}$ difference between $(CH_3)_3SiCl$, $(CH_3)_2SiCl_2$ and CH_3SiCl_3.

The similarities over the latter three methylchlorosilanes is rationalized by postulating that $p\pi - d\pi$ back-bonding occurs from the filled Cl p orbitals to the vacant Si d orbitals. This

effect can curtail the Si → Cl inductive effect(s) to such an extent that a similar overall inductive effect is produced for the intermediate states of the three methylchlorosilanes. Thus the negative character of the H_a atom would be invariant in each case, resulting in a constant polar effect.

However, the chemical shifts for the hydrogen atoms in the methylchlorosilanes are larger than for the methylfluorosilanes which is not in keeping with the postulate of the last paragraph. Possibly anisotropy plays a larger part in determining the chemical shift than electron density. It is worth noting that the differences between the chemical shifts of chloro and fluorosilanes is not nearly so marked[4,23,24].

	chemical shift (p.p.m.)		chemical shift (p.p.m.)
SiH_4	3.20		
SiH_3Cl	4.59	SiH_3F	4.76
SiH_2Cl_2	5.40	SiH_2F_2	4.71
$SiHCl_3$	6.07	$SiHF_3$	4.59

Furthermore, the fact that chlorine abstraction is not observed suggests that the Si-Cl bond is a strong one; $p\pi - d\pi$ interactions would certainly be a positive factor toward bond strengthening. Estimates for the Si-Cl bond strength vary[4] from 82 to 120 kcal. mole^{-1} which is significantly high.

Throughout these studies Ayscough's value for the rate of recombination of $\cdot CF_3$ radicals[21] was used, as was Shepp's value for the similar process involving $\cdot CD_3$ radicals[19]. (The latter had been more recently verified by March and Polanyi[20]).

2.2 Hydrogen Abstraction Reactions from Halosilanes using $\cdot CH_3$ and $\cdot CF_3$ radicals; references 5, 6, 7.

Kerr, Slater and Young worked on the reactions of $\cdot CH_3$ radicals with the chlorosilanes (and methylchlorosilanes). They noted that the reactivity of the silanes was higher com-

pared with the carbon analogues and they accredited this behaviour to high A factors, rather than to low activation energies[5].

However, this work was doubted on the evidence of later work with these systems[6] which showed that the A factors were in the "normal range" of log A = 11.5 - 12.5. Subsequent work by Kerr, Stephens and Young led to amended results.

2.2.1. Results.

	log A	E_A (kcal. mole^{-1})	Reference
$\cdot CH_3 + HSiCl_3$	13.4	8.5	Kerr, Slater, Young[5]
$\cdot CF_3 + HSiCl_3$	12.13	6.85	Bell, Johnson[6]
$\cdot CF_3 + HSiCl_3$	11.77	5.98	Kerr, Stephens, Young[7]
$\cdot CH_3 + HSiCl_3$	10.83	4.30	Kerr, Stephens, Young[7]

2.2.2. Interpretation of Results.

Thus in these systems, the A factors are in, or close to, the normal range, and the higher reactivity of the silanes, compared with the carbon analogues, is reflected in the lower activation energies for hydrogen abstraction.

It is noted that the activation energy for the abstraction of hydrogen from trichlorosilane, $HSiCl_3$, is higher for $\cdot CF_3$ attack, which is the opposite effect to that noted with the methylhalosilanes.

The hydrogen atoms in the methylhalosilanes are hydridic in nature and thus more readily abstracted by the electrophilic $\cdot CF_3$ radical. The hydrogen atom in $HSiCl_3$ is more easily affected by the inductive effect of the Cl atoms than are the methyl hydrogens in the methylhalosilanes. Thus the hydrogen atoms in the halosilanes are probably more protonic in nature.

Therefore, on pure qualitative reasoning one would predict a higher activation energy for the $\cdot CF_3 + HSiCl_3$ system with respect to the $\cdot CF_3 + HSiCl_3$ case.

2.3. Hydrogen Abstraction Reactions from the Group IV Tetramethyls using $\cdot CH_3$, $\cdot CD_3$ and $\cdot CF_3$ Radicals; references 12, 13, 14, 15, 16.

Arrhenius parameters have been recorded for hydrogen abstraction from the tetramethyl compounds of the group IV elements. Some studies have been of four members of the group:

$C(CH_3)_4$, $Si(CH_3)_4$, $Ge(CH_3)_4$, $Sn(CH_3)_4$, with $\cdot CF_3$ radicals, (Bell and Platt[12]).

$Si(CH_3)_4$, $Ge(CH_3)_4$, $Sn(CH_3)_4$, $Pb(CH_3)_4$, with $\cdot CH_3$ radicals, (Chaudhry and Gowenlock[13]).

Other studies have included a comparison of $C(CH_3)_4$ and $Si(CH_3)_4$ using $\cdot CH_3$ and $\cdot CF_3$ radicals, (Morris and Thynne[14]), and a comparison of $Si(CH_3)_4$ with four different radicals, $\cdot CF_3$, $\cdot CH_3$, $\cdot CD_3$ and $\cdot C_2H_5$, (Kerr, Stephens and Young[16]).

2.3.1. Results.

	log A	E_A (kcal. mole^{-1})	log k_H (400°K)
$\cdot CF_3$ + $C(CH_3)_4$*	12.0 ± 0.09	8.37 ± 0.09	7.43
+ $Si(CH_3)_4$	11.9 ± 0.09	7.30 ± 0.14	7.91
+ $Ge(CH_3)_4$	11.7 ± 0.03	7.37 ± 0.03	7.67
+ $Sn(CH_3)_4$	11.7 ± 0.08	7.25 ± 0.07	7.74
	reference: Bell and Platt [12]. *Bell and Zucker [8].		
$\cdot CH_3$ + $Si(CH_3)_4$	12.6 ± 0.19	11.0 ± 0.34	6.59
+ $Ge(CH_3)_4$	11.8 ± 0.21	9.6 ± 0.39	6.56
+ $Sn(CH_3)_4$	11.1 ± 0.13	8.6 ± 0.24	6.40
+ $Pb(CH_3)_4$	10.2 ± 0.48	7.4 ± 0.88	6.16
	reference: Chaudhry and Gowenlock[13].		
$\cdot CH_3$ + $C(CH_3)_4$	12.3	12.0	5.74
	reference: Kerr and Timlin[15].		

$\cdot CF_3$ + $Si(CH_3)_4$	11.90 ± 0.05	7.23 ± 0.09	7.95
$\cdot CH_3$ +	11.55 ± 0.18	10.23 ± 0.36	5.98
$\cdot CD_3$ +	11.84 ± 0.06	10.36 ± 0.12	6.20
$\cdot C_2H_5$ +	11.88 ± 0.22	11.40 ± 0.48	5.68
	reference: Kerr, Stephens and Young[16].		
$\cdot CH_3$ + $C(CH_3)_4$[26]	11.3	10.0	5.84
+ $Si(CH_3)_4$	11.5 ± 0.2	10.3 ± 0.4	5.87
$\cdot CF_3$ + $C(CH_3)_4$[27]	11.8	7.6	7.65
+ $Si(CH_3)_4$	12.0 ± 0.1	7.6 ± 0.2	7.85
	reference: Morris and Thynne[14].		

2.3.2. Interpretation of Results.

An analysis of the data of Bell and Platt[12] gives important information on the relationship between reactivity and electronegativity. A plot of log k_H v. proton chemical shift produces a gentle curve with log k decreasing with increasing chemical shift, in the order $Si(CH_3)_4$, $Sn(CH_3)_4$, $Ge(CH_3)_4$ and $C(CH_3)_4$. (See graph 11). This suggests that the reactivity of the tetramethyl decreases as the Pauling electronegativity increases which is in keeping with the logic that abstraction of hydrogen by the electrophilic $\cdot CF_3$ radical would be more facile with the more hydridic hydrogens. The most hydridic hydrogen would be associated with $Si(CH_3)_4$ as silicon has the lowest electronegativity. This is confirmed by the results.

However, the results of Chaudhry and Gowenlock[13] do not complement the latter results. Their plot of log k_H against the ^{13}C-H coupling constant, $J(^{13}C\text{-}H)$, shows a gentle curve but with the order Si > Ge > Sn > Pb which does not agree with that of Bell and Platt for the $\cdot CF_3$ systems[12], (see overleaf).

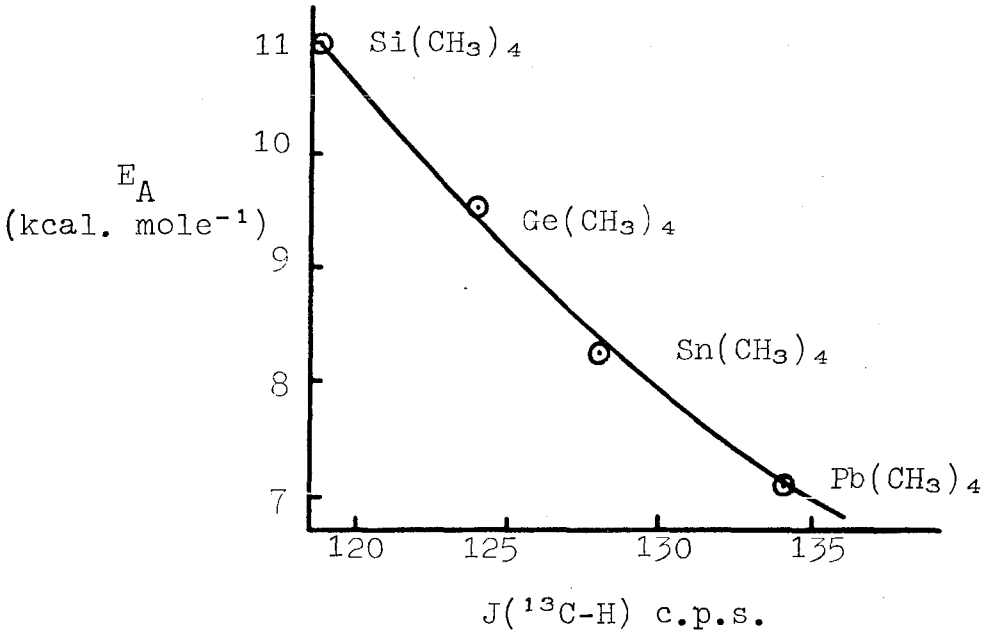
11
10
9
8
7
E_A
(kcal. mole^{-1})
$Si(CH_3)_4$
$Ge(CH_3)_4$
$Sn(CH_3)_4$
$Pb(CH_3)_4$
120
125
130
135
J(^{13}C-H) c.p.s.

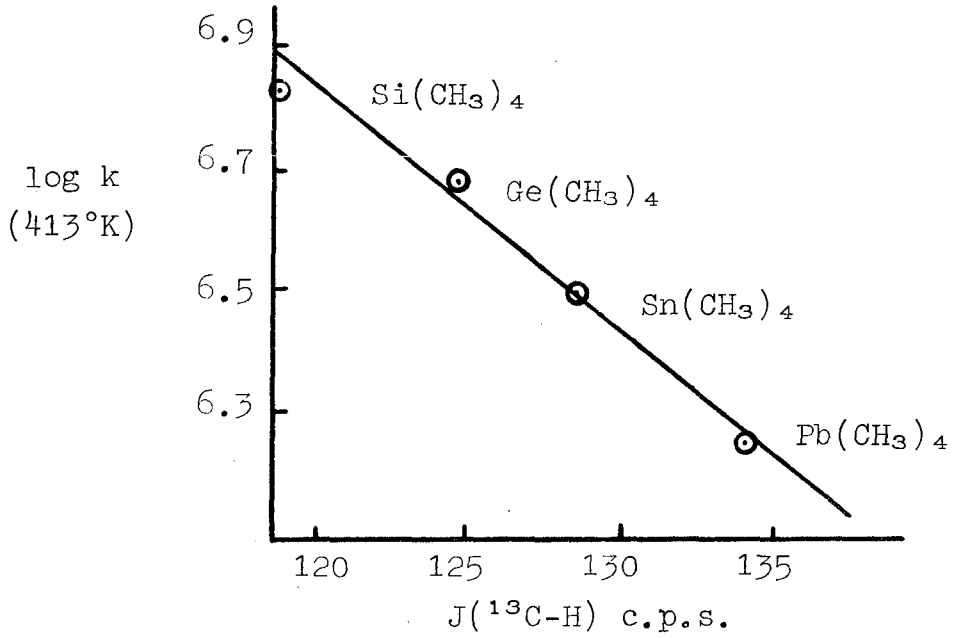
6.9
6.7
6.5
6.3
log k
(413°K)
$Si(CH_3)_4$
$Ge(CH_3)_4$
$Sn(CH_3)_4$
$Pb(CH_3)_4$
120
125
130
135
J(^{13}C-H) c.p.s.

The results of Chaudhry and Gowenlock are doubted on several counts. One would expect an increasing order of log k values compared to the decreasing order of activation energy values, but the orders are the same. This suggests that the A factors may be incorrect. On inspection one can see that the A factors are considerably different, (unlike those of Bell and Platt), and furthermore, nearly all are outside the normal range. The authors make reference to results of Kerr, Slater and Young[5] who later admitted their work to be incorrect on the point of A factors being too high.

It is instructive to add values for the $\cdot CD_3 + C(CH_3)_4$ system to the plots of Chaudhry and Gowenlock. Kerr and Timlin[15] have determined the Arrhenius parameters and McFarlane[25] has determined $J(^{13}C\text{-}H)$ for $C(CH_3)_4$ to be 122 c.p.s.. It is seen clearly that the data for $C(CH_3)_4$ does not fit onto either of the above graphs.

Subsequent work on the $\cdot CH_3 + Si(CH_3)_4$ system by Kerr, Stephens and Young[16] and that by Morris and Thynne[14] shows close agreement between the two groups of workers but some differences to the figures of Chaudhry and Gowenlock.

Sufficient evidence is available to justify a re-investigation of the work of the latter.

Referring again to Morris and Thynne, they have measured the Arrhenius parameters for hydrogen abstraction from $Si(CH_3)_4$ with both $\cdot CH_3$ and $\cdot CF_3$ radicals[14], and compared their findings with some earlier results of the same radicals with $C(CH_3)_4$[26,27].

Morris and Thynne conclude that "for attack by the same radical, the Arrhenius parameters and velocity constants are identical, within experimental error, for neopentane and tetramethylsilane, thus the substitution of the central atom by silicon has little effect upon the reactivity of the adjacent C-H bonds".

This rather dogmatic statement is in disagreement with most other findings in this field of study. The rather old values for $C(CH_3)_4$, chosen for comparison, have been super-

seded. If one takes Kerr and Timlin's values for $\cdot CH_3$ + $C(CH_3)_4$[15] and Bell and Zucker's values for $\cdot CF_3$ + $C(CH_3)_4$[8], then differences are noted for replacement of carbon by silicon for attack by both radicals.

Morris and Thynne's own values for $\cdot CH_3$ and $\cdot CF_3$ attack on $Si(CH_3)_4$ are in fair agreement with those of other workers. In the former case of $\cdot CH_3$ radical attack, the values of the Arrhenius parameters determined by Kerr, Stephens and Young[16] are complementary.

The values for $\cdot CF_3$ radical attack on $Si(CH_3)_4$, obtained by both Kerr et al[16] and Bell and Zucker[8] are in excellent agreement with those of Morris and Thynne.

Therefore, sufficient evidence is at hand to substantiate the qualitative rule that replacement of the central carbon atom does have an effect on the reactivity of the adjacent C-H bonds.

Conclusions can be drawn from the work of Kerr, Stephens and Young[16]. The values of $Si(CH_3)_4$ with both $\cdot CF_3$ and $\cdot CD_3$ radicals compare fairly well with those of Bell and Platt[12]. It was deduced by Kerr et al that an order of reactivities may be stated:

$$\cdot CF_3 > \cdot CH_3 \sim \cdot CD_3 > \cdot C_2H_5$$

It is also noted that this sequence parallels that of bond dissociation energies:

$$D(F_3C\text{-}H) > D(H_3C\text{-}H) > D(H_5C_2\text{-}H)$$

2.4. Secondary Reactions; references 17, 18, 28, 30.

Other reactions have been noted in the reactions of the methylhalosilanes and group IV tetramethyls with $\cdot CD_3$ and $\cdot CF_3$ radicals.

One such reaction is that of hot molecule formation between the abstracted substrate and $\cdot CF_3$ radicals. The hot

molecule either undergoes a β-fluoro rearrangement reaction and elimination, or collisionally deactivates followed by a thermolysis reaction. In both cases CF_2CH_2 is formed.

Both the above reactions occur only when the central metal atom has vacant d orbitals; neither reaction is noted for $C(CH_3)_4$.

When $\cdot CD_3$ radicals are used, the rearrangement-elimination reaction is not possible.

Another reaction, of more pertinent study here, is that of radical exchange which has been noted in earlier work[28,29], and more recently in the reactions of $\cdot CF_3$ radicals with the group IV tetramethyls[17,18] and of $\cdot CD_3$ radicals with $B(CH_3)_3$[30].

In these more recent studies, direct exchange, resulting in the production of $\cdot CH_3$ radicals, has been postulated to account for CH_4, C_2H_6 and CF_3CH_3/CD_3CH_3, (methyl containing products). The absence of such methyl containing products when neopentane is used as a substrate indicates that the availability of empty orbitals, (d orbitals for Si, Sn, Ge; and p orbitals for B), is possibly a crucial factor in the exchange mechanism. Such a mechanism involves an intermediate step where the co-ordination number of the central metal atom is increased.

Quantitative yields were obtained only in the case of $\cdot CF_3$ radicals with $Sn(CH_3)_4$ and the following reactions were proposed:

Radical exchange: $\cdot CF_3 + Sn(CH_3)_4 \rightleftarrows [CF_3 - Sn(CH_3)_4] \rightarrow CF_3 - Sn(CH_3)_3 + \cdot CH_3$ 1.

Abstraction : $\cdot CF_3 + Sn(CH_3)_4 \longrightarrow CF_3H + \cdot CH_2Sn(CH_3)_3$ 2.

$\cdot CH_3 + Sn(CH_3)_4 \longrightarrow CH_4 + \cdot CH_2Sn(CH_3)_3$ 3.

Recombination : $\cdot CF_3 + \cdot CF_3 \longrightarrow C_2F_6$ 4.

$\cdot CH_3 + \cdot CH_3 \longrightarrow C_2H_6$ 5.

$\cdot CH_3 + \cdot CF_3 \longrightarrow CH_3CF_3^* \xrightarrow{M} CH_3CF_3$ 6.

$\cdot CH_3 + \cdot CF_3 \longrightarrow CH_3CF_3^* \longrightarrow CH_2CF_2 + HF$ 7.

For this system Bell and Platt[18] obtained a value of 5.9×10^6 ml m^{-1} s^{-1} for k_3 which compares with Chaudhry and Gowenlock's[13] value of 5×10^6 ml m^{-1} s^{-1}.

Such experimental evidence is in favour of methyl products resulting from $\cdot CH_3$ radicals.

Since the methyl products were not found either by heating a mixture of HFA + $Sn(CH_3)_4$ or by photolyzing $Sn(CH_3)_4$ alone under experimental conditions, the methyl radicals must originate from an exchange process such as that indicated by equation 1.

Although full quantitative analysis was not possible with substrates other than $Sn(CH_3)_4$, estimates of the amounts of CH_4 and C_2H_6 produced lead to the following postulated order of the relative rates of radical exchange:

$$B(CH_3)_3 > Sn(CH_3)_4 >> Ge(CH_3)_4 \sim Si(CH_3)_4$$

3. Research: The Reactions of $\cdot CD_3$ radicals with tetramethylstannane and tetramethylgermane.

3.1. Experimental.

3.1.1. Apparatus.

A greaseless vacuum system was employed. Photolyses were carried out in a quartz Ultrasil cell of 125.4 ml illuminated volume. The cell was fitted with plane end windows and had an appendage centrally situated at right angles to the cell length. The cell was enclosed in a well lagged tubular furnace whose temperature was controlled to ±0.2°C with an R.F.L. platinum resistance proportional controller. Four chromel-alumel thermocouples were used to measure the temperature and were situated symmetrically around the reaction cell. The appendage extended out of and below the furnace and lagging.

The light source used was a P.E.K. 200 W high pressure mercury arc lamp. When acetone-d_6 was used as a source of $\cdot CD_3$ radicals, light of wavelength around 3130 Å was isolated by a Corning filter, CS 754, and standard solutions of nickel and cobalt sulphate, and of potassium hydrogen phthalate[31]. When azomethane-d_6 was used as a radical source, light of wavelength 3660 Å was obtained by using a combination of filters CS 760 and 052, as used by Cheng, Nimoy and Toby[32].

Another section of the apparatus consisted of four small flasks, of which adjacent pairs could be connected by opening a stopcock; each of these flasks could be enveloped by a slush bath. Bulb to bulb distillations and degassing of all materials was effected in this section of the apparatus, prior to storage in blackened bulbs above the reaction vessel.

A standard system of oil rotary and mercury diffusion pumps were used to attain pressures of around 10^{-5} torr or better. The gaseous reaction products were collected by means of the Toepler pump technique described by Gowenlock and Melville[33].

3.1.2. Procedure.

In a typical experiment, the radical source and tetramethyl substrate were admitted separately into the reaction cell from their blackened storage flasks; a Ruska Instrument Company precision quartz spiral gauge was used for pressure measurements. The mixture was frozen down by liquid nitrogen into the appendage and pumped out to less than 10^{-3} torr pressure. The outlets to the pumping system were closed, the cold trap removed, and the appendage warmed by hand to melt the frozen reactants. When the quartz spiral gauge recorded that the pressure had returned to its original value and the reactants had been left to mix and attain the furnace temperature, a photolysis was carried out. The temperature range employed for these experiments was 25 - 150°C inclusive in 25° steps, (with the addition of 137.5°C when HDA was used). When HDA was used as a radical source, a partial pressure of 30 mm was used for both it and the tetramethyl substrate. When HDAM was used then the partial pressure of both it and the substrate was reduced to 20 mm.

In experiments with HDA, a photolysis time of 120 seconds was used at reaction temperatures 150 - 100°C inclusive, 240 seconds at 75°C, 600 seconds at 50°C and 1200 seconds at 25°C. However, when azomethane-d_6 was used, a photolysis time of 120 seconds was found to be sufficient at all temperatures.

After photolyses, the products were collected in a cold trap, which was maintained at -160°C by an isopentane slush bath. This condensed all compounds except methanes and ethanes which were allowed to effuse into a Toepler flask on the opening of a suitable valve. These gaseous products were collected in the capillary tube situated vertically above the flask until the pressure in that section of the apparatus had stabilized at equal to or less than 3×10^{-3} torr. A rubber cup was fitted to a position on the capillary tube such that the addition of liquid nitrogen into the cup froze a plug of mercury, thereby enclosing the sample gases in the tube above

the mercury. The capillary tube was then sealed below the mercury plug and removed. Another capillary tube was then glass-blown on in its place for the next experiment and the whole apparatus pumped out to remove the condensables.

The sample tubes collected thus, were placed in a suitable device in the inlet system of a gas chromatography apparatus or mass spectrometer (Hitachi RMU 6E) according to the data required. Gas chromatographic analysis gave the rates of production from photolysis of both methane and ethane from which the ratios of total methane to ethane were calculated for each temperature. Mass spectrometric analysis was used to determine the CD_3H : CD_4 ratio (19 : 20 mass peaks) and to look at the 30 - 36 mass range to elucidate the amount of radical exchange.

3.1.3 Materials and their Purification.

3.1.3.1. Hexadeuteroacetone.

This was obtained from Stohler Isotope Chemicals. Mass spectrometric analysis showed that the sole impurity was CD_2HCOCD_3 present to about 5%.

3.1.1.2. Hexadeuteroazomethane.

This was obtained from Merck, Sharp and Dohme Ltd. of Montréal. Mass spectrometric analysis showed various peaks of mass number greater than 64, at 70, 78, 112, 131, 147 and 185, notably that at 147.

After reference to previous distillations[32,34,35,36], the material was purified by distillation using traps at -98°, -131.5° and -196°C, using slush baths of methanol and isopentane for the first two traps, and liquid nitrogen for the third. After two hours the small tail fraction collecting at -98°C was rejected and the major fraction collecting at -131.5°C was re-distilled for a further two and a half hours. The major fraction was collected again at -131.5°C and transferred

directly to a blackened storage bulb situated above the reaction cell. The very small fraction at -98°C was combined with that from the first distillation. In neither distillation was any material collected at -196°C.

A subsequent mass spectrometric analysis of the -131.5°C fraction showed no mass peak greater than 64. However, there was a small peak at 63; the ratio of 64 : 63 was 39.5 : 3.45. If all the 63 peak corresponds to $CD_2HN_2CD_3$ then azomethane was 91.97% AZM-d_6 and 8.03% AZM-d_5.

3.1.3.3. Tetramethylstannane, $Sn(CH_3)_4$.

This was obtained from Alpha Inorganics Ltd. and distilled three times using traps at -98° and -131.5°. The fraction collecting at -98° after the third distillation was thoroughly degassed and stored in a blackened storage bulb above the reaction cell.

3.1.3.4. Tetramethylgermane, $Ge(CH_3)_4$.

A procedure identical to that of tetramethylstannane was employed.

3.2. Hydrogen Abstraction using Hexadeuteroacetone.

3.2.1. Kinetics.

Using hexadeuteroacetone (HDA) as a radical source, the following processes were involved. (The HDA was found to contain 5% CD_2HCOCD_3 as impurity.)

Photolysis: $CD_3COCD_3 \xrightarrow{h\nu} 2{}^{\bullet}CD_3 + CO$ 1a.

$CD_2HCOCD_3 \xrightarrow{h\nu} {}^{\bullet}CD_2H + {}^{\bullet}CD_3 + CO$ 1b.

Abstraction of a hydrogen atom from the tetramethyl substrate to yield CD_3H:

$$\cdot CD_3 + M(CH_3)_4 \xrightarrow{k_2} CD_3H + \cdot CH_2M(CH_3)_3 \qquad 2.$$

where M = Sn or Ge.

Additional abstraction reactions within the radical source itself are:

$$\cdot CD_3 + CD_3COCD_3 \xrightarrow{k_3} CD_4 + \cdot CD_2COCD_3 \qquad 3.$$

$$\cdot CD_3 + CD_2HCOCD_3 \xrightarrow{k_4'} CD_3H + \cdot CD_2COCD_3 \qquad 4'.$$

$$\cdot CD_2H + CD_3COCD_3 \xrightarrow{k_4''} CD_3H + \cdot CD_2COCD_3 \qquad 4''.$$

Recombination:

$$\cdot CD_3 + \cdot CD_3 \xrightarrow{k_5} C_2D_6 \qquad 5.$$

$$\cdot CD_2H + \cdot CD_3 \xrightarrow{k_6'} C_2D_5H \qquad 6'.$$

$$\cdot CD_2H + \cdot CD_2H \xrightarrow{k_6''} C_2D_4H_2 \qquad 6''.$$

Mass spectrometric analysis showed that R_6' was very small and R_6'' not detectable.

Photolysis of HDA alone.

Gas-liquid chromatographic and mass spectrometric analysis was employed to obtain values of $k_3/k_5^{\frac{1}{2}}$, at each temperature, which are subsequently used to evaluate $k_2/k_5^{\frac{1}{2}}$.

From G.L.C. analysis: $$\frac{Ra_{methane}}{R_{C_2D_6}^{\frac{1}{2}}} \qquad (A)$$

From mass spectrometric analysis: $$\frac{R_{CD_4}}{R_{CD_4} + R_{CD_3H}} \qquad (B)$$

(A) x (B): $$\frac{Ra_{methane}}{R_{C_2D_6}^{\frac{1}{2}}} \times \frac{R_{CD_4}}{R_{CD_4} + R_{CD_3H}} = \frac{Ra_{CD_4}}{R_{C_2D_6}^{\frac{1}{2}}}$$

now $$\frac{Ra_{CD_4}}{R_{C_2D_6}^{\frac{1}{2}}} \times \frac{1}{[\text{acetone-}d_6]} = \frac{k_3}{k_5^{\frac{1}{2}}} \qquad (C)$$

Photolysis of HDA plus substrate.

Mass spectrometric analysis only was needed, to obtain the ratio of the total rates of formation of CD_3H : CD_4, ($^{Rt}CD_3H$: $^{Rt}CD_4$).

Thus $\frac{^{Rt}CD_3H}{^{Rt}CD_4} =$

$$\frac{k_2\,[CD_3][\text{substrate}] + k_4'\,[CD_3][Ac\text{-}d_5] + k_4''\,[CD_2H][Ac\text{-}d_6]}{k_3[CD_3][Ac\text{-}d_6]}$$

$$= \frac{k_2\,[\text{substrate}]}{k_3\,[Ac\text{-}d_6]} + \frac{k_4'\,[Ac\text{-}d_5]}{k_3\,[Ac\text{-}d_6]} + \frac{k_4''\,[CD_2H]}{k_3\,[CD_3]} \qquad (D)$$

(Ac = acetone)
but from the photolysis of acetone alone:

$$\frac{^{Ra}CD_3H}{^{Ra}CD_4} = \frac{k_4'\,[CD_3][Ac\text{-}d_5] + k_4''\,[CD_2H][Ac\text{-}d_6]}{k_3\,[CD_3][Ac\text{-}d_6]}$$

$$= \frac{k_4'\,[Ac\text{-}d_5]}{k_3\,[Ac\text{-}d_6]} + \frac{k_4''\,[CD_2H]}{k_3\,[CD_3]} \qquad (E)$$

now, neither $\frac{[Ac\text{-}d_5]}{[Ac\text{-}d_6]}$ nor $\frac{[CD_2H]}{[CD_3]}$ depend on [substrate],

thus (E) may be subtracted from (D):

$$\frac{^{Rt}CD_3H}{^{Rt}CD_4} - \frac{^{Ra}CD_3H}{^{Ra}CD_4} = \frac{k_2\,[\text{substrate}]}{k_3\,[Ac\text{-}d_6]}$$

$$\text{thus } \frac{k_2}{k_3} = \frac{[Ac\text{-}d_6]}{[\text{substrate}]} \times \left[\frac{^{Rt}CD_3H}{^{Rt}CD_4} - \frac{^{Ra}CD_3H}{^{Ra}CD_4}\right] \qquad (F)$$

$$\text{now } \frac{k_2}{k_5^{\frac{1}{2}}} = \frac{k_2}{k_3} \times \frac{k_3}{k_5^{\frac{1}{2}}}$$

values of $k_3/k_5^{\frac{1}{2}}$ are obtained from the photolysis of HDA alone, (C), and thus:

$$\frac{k_2}{k_5^{\frac{1}{2}}} = \frac{[\text{Ac-d}_6]}{[\text{substrate}]} \times \left[\frac{Rt_{CD_3H}}{Rt_{CD_4}} - \frac{Ra_{CD_3H}}{Ra_{CD_4}}\right] \times \frac{k_3}{k_5^{\frac{1}{2}}} \qquad (G)$$

Since the hexadeuteroacetone (HDA) used was 95% Ac-d_6 and equal partial pressures of HDA and substrate were used, $\frac{[\text{Ac-d}_6]}{[\text{substrate}]} = 0.95$.

3.2.2. Results.

3.2.2.1. Photolysis of Hexadeuteroacetone alone.

Most of the gas liquid chromatographic analysis was performed by Dr. A. E. Platt for concurrent work[30] and the values given are listed in Table 1 and subscripted (AEP). Two samples obtained at 150°C were analyzed in the same way to check this work. Also two samples were obtained at 137.5°C. The full complement of results are also reported for the latter four samples in Table 1.

Mass spectrometric analysis of the mass peaks at 19 and 20 produced the CD_3H : CD_4 and CD_3H : Total methane (CD_3H + CD_4) at each temperature and five pairs of figures for the 19 and 20 peaks obtained from the mass spectrometer for each sample. See Table 2.

Table 1. Photolysis of HDA alone; Mass Spectrometric Analysis for Mass Peaks 19 and 20.

Temps °C		$\frac{19}{20} = \frac{Ra_{CD_3H}}{Ra_{CD_4}}$ (average)		$\frac{Ra_{CD_3H}}{Ra_{CD_4}}$ (mean of average values)
150	(c)	0.103		0.103
137.5	(a)	0.158	}	0.164
137.5	(b)	0.169		
125	(a)	0.213		0.213
100	(a)	0.241		0.241
75	(a)	0.200		0.200
50	(b)	0.120	}	0.109
50	(c)	0.097		
25	(b)	0.090	}	0.087
25	(c)	0.084		

Table 2. Results of the Photolysis of Acetone alone.

Temp. °C	$\frac{Ra_{methane}}{R^{\frac{1}{2}}_{C_2D_6}}$ (*) x 10^7	$\frac{R_{CD_4}}{R_{(CD_4 + CD_3H)}}$	$\frac{Ra_{CD_4}}{R^{\frac{1}{2}}_{C_2D_6}}$ (*) x 10^7	[Acetone] d_6 (m ml^{-1}) x 10^7	$\frac{k_3}{k^{\frac{1}{2}}_5}$ (‡)	log $\frac{k_3}{k^{\frac{1}{2}}_5}$
150(AEP)		$\frac{1}{1.103}$		10.80	0.1322	$\bar{1}$.1212	-0.8788
150 (a)	1.505	$\frac{1}{1.103}$	1.369	10.80	0.1263	$\bar{1}$.1014	-0.8986
150 (b)	1.669	$\frac{1}{1.103}$	1.512	10.80	0.1401	$\bar{1}$.1464	-0.8536
137.5(d)	0.9687	$\frac{1}{1.163}$	0.8330	11.12	0.07480	$\bar{2}$.8739	-1.1261
137.5(f)	0.9837	$\frac{1}{1.163}$	0.8459	11.12	0.07600	$\bar{2}$.8808	-1.1192
125(AEP)		$\frac{1}{1.213}$		11.48	0.04855	$\bar{2}$.6861	-1.3139
100(AEP)		$\frac{1}{1.241}$		12.28	0.01912	$\bar{2}$.2814	-1.7186
75(AEP)		$\frac{1}{1.200}$		13.13	0.01057	$\bar{2}$.0240	-1.9760
50(AEP)		$\frac{1}{1.108}$		14.15	0.004920	$\bar{3}$.6920	-2.3080
25(AEP)		$\frac{1}{1.087}$		15.63	0.002963	$\bar{3}$.4717	-2.5283

Table 2. Continued

* : units are $m^{\frac{1}{2}}ml^{-\frac{1}{2}}s^{-\frac{1}{2}}$

‡ : units are $ml^{\frac{1}{2}}m^{-\frac{1}{2}}s^{-\frac{1}{2}}$

The 150(a) and 150(b) results average out to essentially the same value as 150(AEP). Therefore, the latter value was taken, for consistency. The values at 137.5°C were averaged to give $k_3/k_5^{\frac{1}{2}}$ = 0.07540 for use later.

Graph 1. Photolysis of HDA alone.

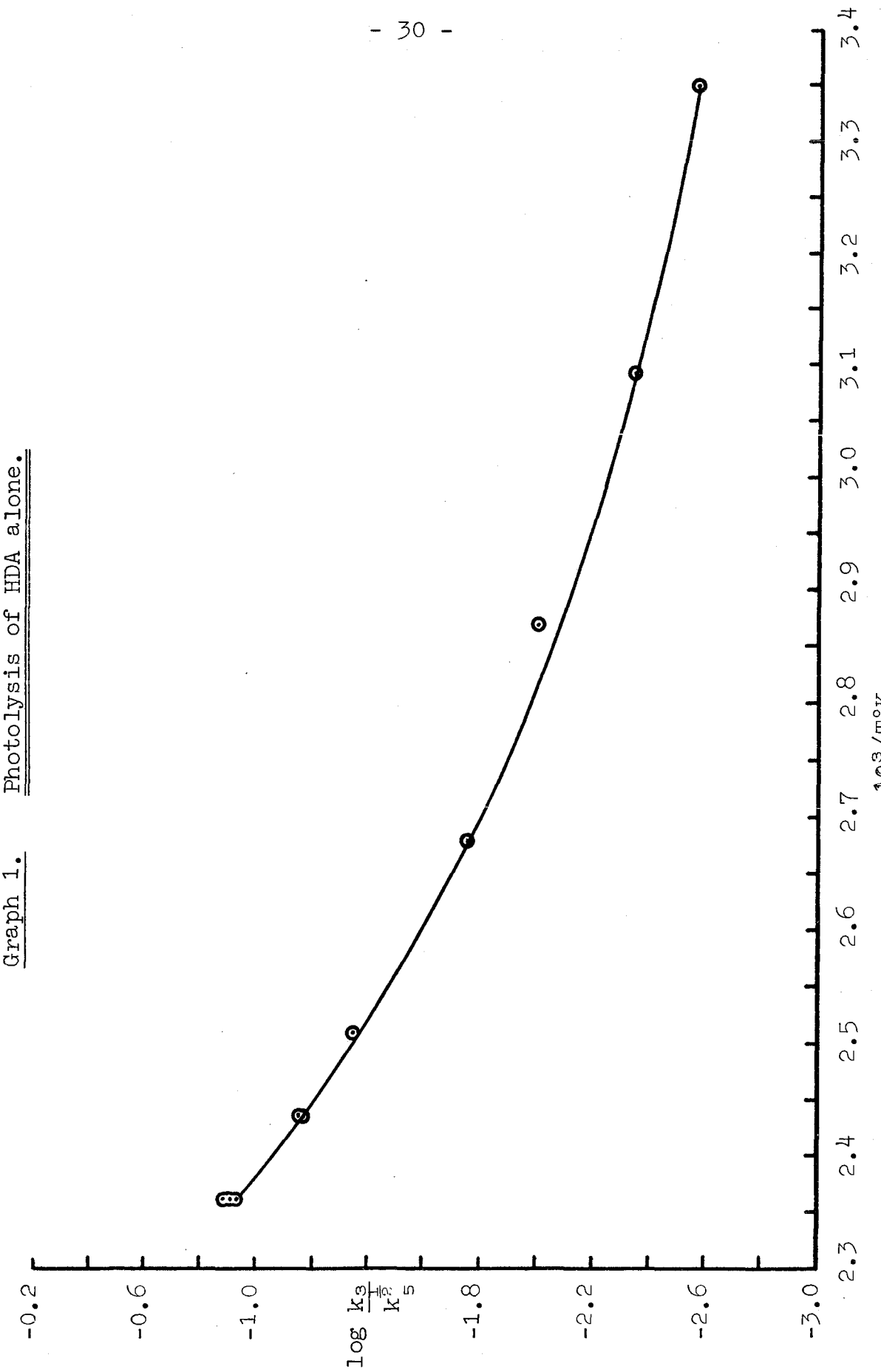

3.2.2.2. Photolysis of Hexadeuteroacetone with Tetramethylstannane.

Mass spectrometric analysis for the mass peaks 19 and 20 was obtained at each temperature. Several samples were obtained at each temperature with five pairs of figures for the 19 and 20 peaks obtained from the mass spectrometer for each sample. See Table 3.

Values of $k_2/k_5^{\frac{1}{2}}$ in equation G in section 3.2.1. were obtained at each temperature by the method described in section 3.2.1. utilizing values of $k_3/k_5^{\frac{1}{2}}$ from Table 1. For calculations see Table 4.

The Arrhenius parameters for the abstraction of hydrogen from the substrate were evaluated from the standard Arrhenius plot and least squares evaluation of the raw data.

Table 3. Photolysis of HDA + $Sn(CH_3)_4$; Mass Spectrometric Analysis for Mass Peaks 19 and 20.

Temps °C	$\frac{19}{20} = \frac{Rt_{CD_3H}}{Rt_{CD_4}}$
150 (a)	3.780
150 (b)	4.320
150 (c)	5.075
137 (a)	4.340
137 (b)	4.980
125 (a)	4.530
125 (b)	4.350
125 (c)	4.250
100 (a)	3.640
100 (b)	3.910
75 (a)	2.850
75 (b)	1.890
75 (c)	1.780
50 (a)	1.750
50 (b)	1.420
25 (a)	0.910
25 (b)	0.604
25 (c)	0.631

Table 4. Results of the Photolysis of HDA and $Sn(CH_3)_4$.

Temp. °C	$\frac{Rt_{CD_3H}}{Rt_{CD_4}}$	$\frac{Ra_{CD_3H}}{Ra_{CD_4}}$	$\frac{R_{CD_3H}}{R_{CD_4}}$ (corrected)	$\frac{k_3}{k_5^{\frac{1}{2}}}$ ($ml^{\frac{1}{2}}m^{-\frac{1}{2}}s^{-\frac{1}{2}}$)	$\frac{k_2}{k_5^{\frac{1}{2}}}$ ($ml^{\frac{1}{2}}m^{-\frac{1}{2}}s^{-\frac{1}{2}}$)	log $\frac{k_2}{k_5^{\frac{1}{2}}}$	
150 (a)	3.780	0.103	3.677	0.1322	0.4618	$\bar{1}$.6645	-0.3355
150 (b)	4.320	0.103	4.217	0.1322	0.5297	$\bar{1}$.7240	-0.2760
150 (c)	5.075	0.103	4.972	0.1322	0.6246	$\bar{1}$.7956	-0.2044
137.5(a)	4.340	0.164	4.176	0.07540	0.2988	$\bar{1}$.4755	-0.5245
137.5(b)	4.980	0.164	4.816	0.07540	0.3446	$\bar{1}$.5374	-0.4626
125 (a)	4.530	0.213	4.317	0.04855	0.1991	$\bar{1}$.2992	-0.7008
125 (b)	4.350	0.213	4.137	0.04855	0.1908	$\bar{1}$.2807	-0.7193
125 (c)	4.250	0.213	4.037	0.04855	0.1862	$\bar{1}$.2701	-0.7299
100 (a)	3.640	0.241	3.399	0.01912	0.06172	$\bar{2}$.7904	-1.2096
100 (b)	3.910	0.241	3.669	0.01912	0.06662	$\bar{2}$.8236	-1.1764
100 (c)	3.510	0.241	3.269	0.01912	0.05934	$\bar{2}$.7734	-1.2266
75 (a)	2.850	0.200	2.650	0.01057	0.02656	$\bar{2}$.4242	-1.5758
75 (b)	1.890	0.200	1.690	0.01057	0.01693	$\bar{2}$.2289	-1.7711
75 (c)	1.780	0.200	1.580	0.01057	0.01584	$\bar{2}$.1997	-1.8003
50 (a)	1.750	0.109	1.641	0.00492	0.007676	$\bar{3}$.8851	-2.1149
50 (b)	1.420	0.109	1.311	0.00492	0.006132	$\bar{3}$.7876	-2.2124
25 (a)	0.910	0.087	0.823	0.002963	0.002319	$\bar{3}$.3654	-2.6346
25 (b)	0.604	0.087	0.517	0.002963	0.001526	$\bar{3}$.1835	-2.8165
25 (c)	0.631	0.087	0.544	0.002963	0.001533	$\bar{3}$.1856	-2.8144

Table 4 (a). HDA + $Sn(CH_3)_4$: Arrhenius Plot (graph 2)

The values of $k_2/k_5^{\frac{1}{5}}$ at each temperature were averaged out apart from the value of -2.6346 at 25°C which was ignored. A least squares analysis was used to determine the Arrhenius parameters.

Temps $(10^3/T\ °K)$	$\log \frac{k_2}{k_5^{\frac{1}{5}}}$
2.363	-0.2720
2.436	-0.4936
2.512	-0.7167
2.680	-1.2042
2.872	-1.7157
3.094	-2.1637
3.354	-2.8155

Graph 2. Photolysis of HDA + $Sn(CH_3)_4$: Arrhenius Parameters for H Abstraction

Activation Energy 11.65 ± 0.35 kcal. mole^{-1}
log A 12.36 ± 0.21
log k (400°K) 5.99

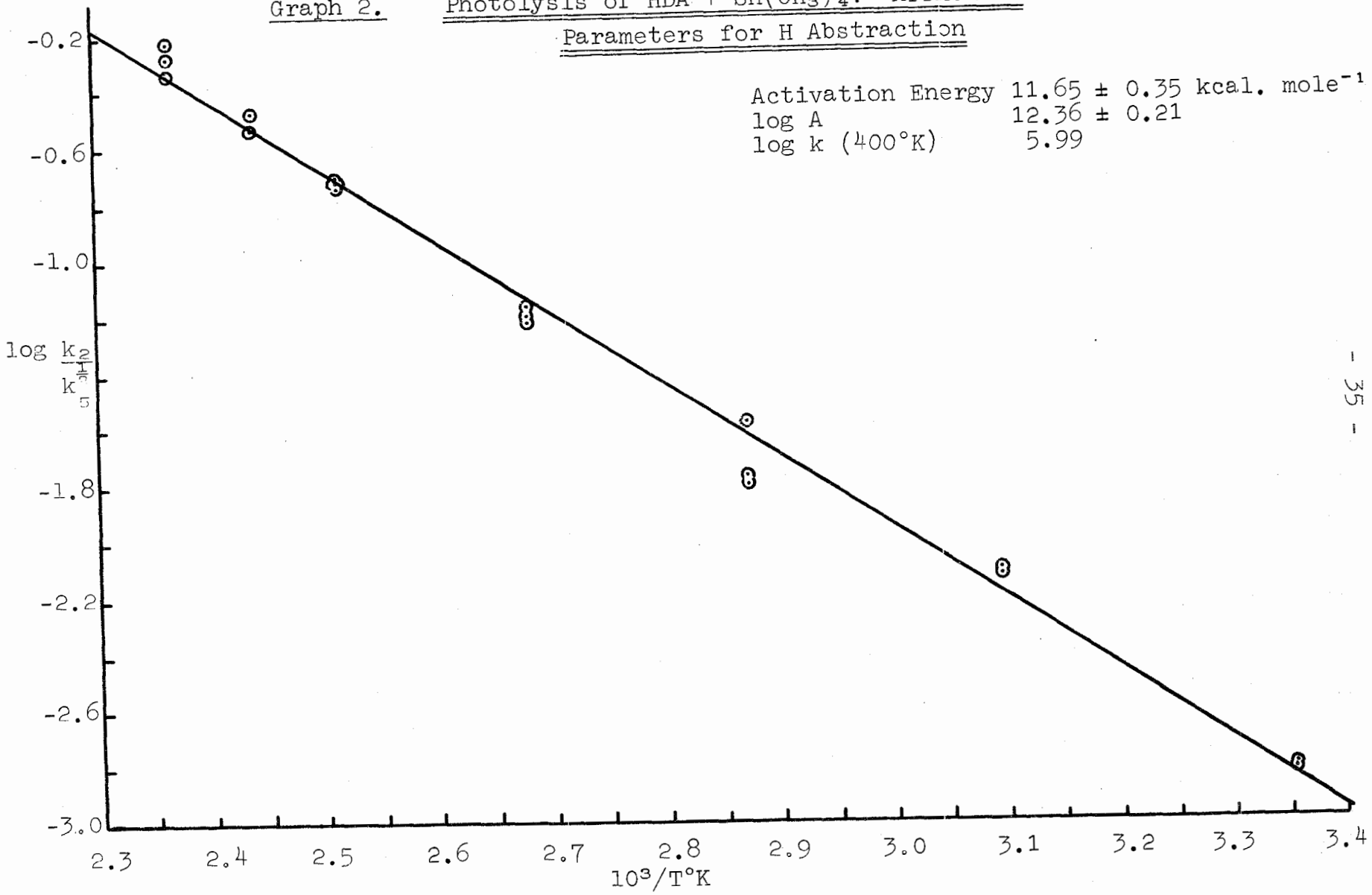

3.2.2.3 Photolysis of Hexadeuteroacetone and Tetramethylgermane.

Mass spectrometric analysis was performed in an identical manner to that described in Section 3.2.2.2. using $Sn(CH_3)_4$ substrate. The Arrhenius parameters were subsequently evaluated for the abstraction of hydrogen from $Ge(CH_3)_4$ using the standard Arrhenius plot and a least squares treatment of the raw data.

Table 5. Photolysis of HDA + $Ge(CH_3)_4$; Mass Spectrometric-Analysis for Mass Peaks 19 and 20.

Temp. °C		$\frac{19}{20} = \frac{Rt_{CD_3H}}{Rt_{CD_4}}$
150	(a)	2.975
150	(b)	2.773
150	(c)	3.568
137.5	(a)	2.898
137.5	(b)	3.011
125	(b)	2.801
125	(c)	2.928
125	(d)	3.723
125	(e)	4.183
125	(f)	3.750
100	(b)	3.151
100	(c)	3.026
100	(d)	3.043
75	(b)	2.091
75	(c)	2.990
75	(e)	3.430
75	(f)	3.338
50	(b)	1.518
50	(c)	1.139
50	(d)	1.630
25	(b)	0.726
25	(c)	0.819
25	(d)	1.046

Table 6. Results of the Photolysis of HDA and $Ge(CH_3)_4$.

Temp. °C	$\frac{Rt_{CD_3H}}{Rt_{CD_4}}$	$\frac{Ra_{CD_3H}}{Ra_{CD_4}}$	$\frac{R_{CD_3H}}{R_{CD_4}}$ (corrected)	$\frac{k_3}{k_5^{\frac{1}{2}}}$ (ml $m^{-\frac{1}{2}}s^{-\frac{1}{2}}$)	$\frac{k_2}{k_5^{\frac{1}{2}}}$ ($ml^{\frac{1}{2}}m^{-\frac{1}{2}}s^{-\frac{1}{2}}$)		log $\frac{k_2}{k_5^{\frac{1}{2}}}$
150 (a)	2.975	0.103	2.872	0.1322	0.3607	$\bar{1}$.5572	-0.4428
150 (b)	2.773	0.103	2.670	0.1322	0.3354	$\bar{1}$.5255	-0.4745
150 (c)	3.568	0.103	3.465	0.1322	0.4352	$\bar{1}$.6387	-0.3613
137.5 (a)	2.898	0.164	2.734	0.07540	0.1957	$\bar{1}$.2916	-0.7084
137.5 (b)	3.011	0.164	2.847	0.07540	0.2038	$\bar{1}$.3092	-0.6908
125 (b)	2.801	0.213	2.588	0.04855	0.1194	$\bar{1}$.0770	-0.9230
125 (c)	2.928	0.213	2.715	0.04855	0.1252	$\bar{1}$.0978	-0.9022
125 (d)	3.723	0.213	3.510	0.04855	0.1619	$\bar{1}$.2093	-0.7907
125 (e)	4.183	0.213	3.970	0.04855	0.1831	$\bar{1}$.2628	-0.7372
125 (f)	3.750	0.213	3.537	0.04855	0.1632	$\bar{1}$.2127	-0.7873
100 (b)	3.151	0.241	2.910	0.01912	0.05283	$\bar{2}$.7229	-1.2771
100 (c)	3.026	0.241	2.785	0.01912	0.05056	$\bar{2}$.7038	-1.2962
100 (d)	3.043	0.241	2.802	0.01912	0.05088	$\bar{2}$.7065	-1.2935
75 (b)	2.091	0.200	1.891	0.01057	0.01895	$\bar{2}$.2777	-1.7223
75 (d)	2.990	0.200	2.790	0.01057	0.02797	$\bar{2}$.4466	-1.5534
75 (e)	3.430	0.200	3.230	0.01057	0.03238	$\bar{2}$.5102	-1.4898
75 (f)	3.338	0.200	3.138	0.01057	0.03145	$\bar{2}$.4976	-1.5024

Table 6. Continued

50	(b)	1.518	0.109	1.409	0.00492	0.006541	$\bar{3}$.8189	-2.1811
50	(c)	1.139	0.109	1.030	0.00492	0.004817	$\bar{3}$.6828	-2.3172
50	(d)	1.630	0.109	1.521	0.00492	0.007114	$\bar{3}$.8521	-2.1579
25	(b)	0.726	0.087	0.639	0.002963	0.001801	$\bar{3}$.2555	-2.7445
25	(c)	0.819	0.087	0.732	0.002963	0.002063	$\bar{3}$.3145	-2.6855
25	(d)	1.046	0.087	0.959	0.002963	0.002703	$\bar{3}$.4318	-2.5682

Table 6 (a). HDA + $Ge(CH_3)_4$: Arrhenius Plot (graph 3).

The values of $k_2/k_5^{\frac{1}{2}}$ at each temperature were averaged out and a least squares analysis was used to determine the Arrhenius parameters.

Temps ($10^3/T$ °K)	$\log \frac{k_2}{k_5^{\frac{1}{2}}}$
2.363	-0.4266
2.436	-0.6996
2.512	-0.8281
2.680	-1.2889
2.872	-1.5670
3.094	-2.2187
3.354	-2.6661

Graph 3. Photolysis of HDA + $Ge(CH_3)_4$: Arrhenius Parameters for H Abstraction.

Activation Energy 10.24 ± 0.43 kcal. mole^{-1}
log A 11.46 ± 0.26
log k (400°K) 5.86

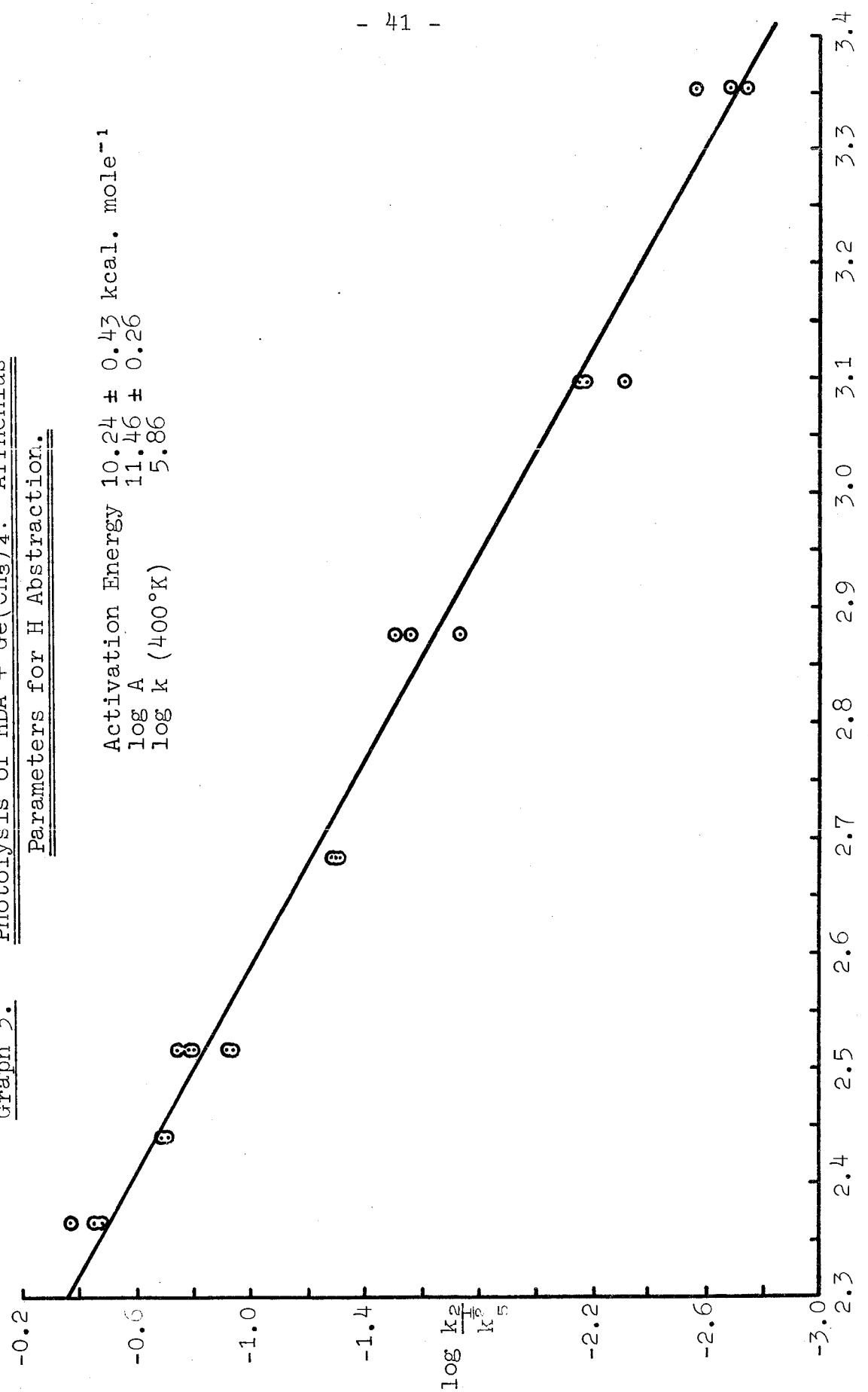

3.3. Hydrogen Abstraction using Hexadeuteroazomethane.

3.3.1. Kinetics.

When hexadeuteroazomethane (HDAM) was used as a radical source, some additional processes have to be taken into account. Some 8% $CD_2HN = NCD_3$ impurity was found by mass spectrometric analysis.

Photolysis:

$$CD_3N{=}{=}NCD_3 \xrightarrow{h\nu} 2{\cdot}CD_3 + N_2 \qquad 1a.$$

$$CD_2HN{=}{=}NCD_3 \xrightarrow{h\nu} {\cdot}CD_2H + {\cdot}CD_3 + N_2 \qquad 1b.$$

$$CD_3N{=}{=}NCD_3 \xrightarrow{h\nu} C_2D_6 + N_2 \qquad 1c.$$

The latter process was noted by previous workers who used azomethane ($CH_3N = NCH_3$), and a quantum yield of 1.0 ± 0.1 has been reported for the formation of nitrogen [35,37]. Thus it was concluded that there was no evidence that collisional deactivation competed with the dissociation processes for the electronically excited azomethane molecules under normal conditions. James and Suart[34] find these conclusions consistent with their own work which shows that the quantum yield of all the processes of 1 are independent of temperature between their working temperatures of 63° and 218°C.

Abstraction of hydrogen occurs from the tetramethyl substrate yielding CD_3H:

$${\cdot}CD_3 + M(CH_3)_4 \xrightarrow{k_2} CD_3H + {\cdot}CH_2M(CH_3)_4 \qquad 2.$$

where M = Sn or Ge.

(assuming ${\cdot}CD_2H$ radicals do not contribute significantly).

Additional abstraction reactions occur from the radical source, as with HDA, to yield CD_3H and CD_4:

$$\cdot CD_3 + CD_3N{=}{=}NCD_3 \xrightarrow{k_3} CD_4 + \cdot CD_2N{=}{=}NCD_3 \quad 3.$$
$$\cdot CD_3 + CD_2HN{=}{=}NCD_3 \xrightarrow{k_4'} CD_3H + \cdot CD_2N{=}{=}NCD_3 \quad 4'.$$
$$\cdot CD_2H + CD_3N{=}{=}NCD_3 \xrightarrow{k_4''} CD_3H + \cdot CD_2N{=}{=}NCD_3 \quad 4''.$$

Recombination:

$$\cdot CD_3 + \cdot CD_3 \xrightarrow{k_5} C_2D_6 \quad 5.$$
$$\cdot CD_2H + \cdot CD_3 \xrightarrow{k_6'} C_2D_5H \quad 6'.$$
$$\cdot CD_2H + \cdot CD_2H \xrightarrow{k_6''} C_2D_4H_2 \quad 6''.$$

Reaction 5 was shown by mass spectrometric analysis to be by far the major process of the latter three.

Addition of $\cdot CD_3$ radicals to the double bond is also possible:

$$\cdot CD_3 + CD_3N{=}{=}NCD_3 \rightarrow (CD_3)_2N\text{-}\dot{N}CD_3 \quad 7.$$

James and Suart suggested that a sufficient excess of $\cdot CD_3$ radicals would remove the radical products of reactions 3, 4, and 7 by radical combination processes:

$$\cdot CD_3 + CD_2N{=}{=}NCD_3 \rightarrow CD_3CD_2N{=}{=}NCD_3 \quad 8.$$
$$\cdot CD_3 + (CD_3)_2N{-}{-}\dot{N}CD_3 \rightarrow (CD_3)_2N{-}{-}N(CD_3)_2 \quad 9.$$

All these processes may be accounted for by an allowance in the overall rate equation. The latter is slightly different to that used for HDA. An allowance has to be made for the ethane produced by the intramolecular elimination process 1c, thus:

$$\frac{k_2[HDAM]}{k_5^{\frac{1}{2}}} = \frac{R_{methane}}{(R_{(Total)C_2D_6} - R_{(1c)C_2D_6})^{\frac{1}{2}}} \quad 10.$$

$R_{(1c)C_2D_6}$ is related to $R_{(1c)N_2}$ which is a fraction of the total nitrogen produced. Some workers have used the approximation $R_{(1c)N_2} = 0.007R_{(Total)N_2}$[2,32,38] but James and Suart derive a coefficient of 0.012 from their expression.

$$\log \Phi_{1c} = \log[2R_{C_2H_6}/(R_{CH_4} + 2R_{C_2H_6})] = \bar{2}.08 \pm 0.4 \qquad 11.$$

The quantum yield for the primary process of intramolecular elimination of ethane was obtained by using cyclohexa-1,4,-diene for quantitative scavenging of the methyl radicals produced by the radical generating processes 1a and 1b.

The coefficient 0.012 was used in connexion with HDAM in the work described here.

Photolysis of HDAM alone.

Gas-liquid chromatographic and mass spectrometric analysis was employed to obtain values of $k_3/k_5^{\frac{1}{2}}$, at each temperature, which are subsequently used to evaluate $k_2/k_5^{\frac{1}{2}}$.

From G.L.C. analysis: $\dfrac{Ra_{methane}}{{}^*R_{C_2D_6}^{\frac{1}{2}}}$ (A)

where ${}^*R_{C_2D_6} = {}^{R}C_2D_6 - 0.012R_{N_2}$

From mass spectrometric analysis: $\dfrac{R_{CD_4}}{R_{CD_4} + R_{CD_3H}}$ (B)

(A) x (B): $\dfrac{Ra_{methane}}{{}^*R_{C_2D_6}^{\frac{1}{2}}} \times \dfrac{R_{CD_4}}{R_{CD_4} + R_{CD_3H}} = \dfrac{Ra_{CD_4}}{{}^*R_{C_2D_6}^{\frac{1}{2}}}$

now $\dfrac{Ra_{CD_4}}{{}^*R_{C_2D_6}^{\frac{1}{2}}} \times \dfrac{1}{[AZM\text{-}d_6]} = \dfrac{k_3}{k_5^{\frac{1}{2}}}$ (C)

Photolysis of HDAM plus substrate.

Mass spectrometric analysis only was needed, to obtain the ratio of the total rates of formation of CD_3H : CD_4, $(Rt_{CD_3H} : Rt_{CD_4})$.

Thus $\frac{Rt_{CD_3H}}{Rt_{CD_4}} =$

$$\frac{k_2\,[CD_3][\text{substrate}] + k_4'\,[CD_3][AZM\text{-}d_5] + k_4''\,[CD_2H][AZM\text{-}d_6]}{k_3[CD_3][AZM\text{-}d_6]}$$

$$= \frac{k_2\,[\text{substrate}]}{k_3\,[AZM\text{-}d_6]} + \frac{k_4'\,[AZM\text{-}d_5]}{k_3\,[AZM\text{-}d_6]} + \frac{k_4''\,[CD_2H]}{k_3\,[CD_3]} \qquad (D)$$

(AZM = azomethane)

but from the photolysis of HDAM alone:

$$\frac{Ra_{CD_3H}}{Ra_{CD_4}} = \frac{k_4'\,[CD_3][AZM\text{-}d_5] + k_4''\,[CD_2H][AZM\text{-}d_6]}{k_3\,[CD_3][AZM\text{-}d_6]}$$

$$= \frac{k_4'\,[AZM\text{-}d_5]}{k_3\,[AZM\text{-}d_6]} + \frac{k_4''\,[CD_2H]}{k_3\,[CD_3]} \qquad (E)$$

now, neither $\frac{[AZM\text{-}d_5]}{[AZM\text{-}d_6]}$ nor $\frac{[CD_2H]}{[CD_3]}$ depend on [substrate],

thus (E) may be subtracted from (D):

$$\frac{Rt_{CD_3H}}{Rt_{CD_4}} - \frac{Ra_{CD_3H}}{Ra_{CD_4}} = \frac{k_2\,[\text{substrate}]}{k_3\,[AZM\text{-}d_6]}$$

$$\text{thus } \frac{k_2}{k_3} = \frac{[AZM\text{-}d_6]}{[\text{substrate}]} \times \left[\frac{Rt_{CD_3H}}{Rt_{CD_4}} - \frac{Ra_{CD_3H}}{Ra_{CD_4}}\right] \qquad (F)$$

$$\text{now } \frac{k_2}{k_5^{\frac{1}{2}}} = \frac{k_2}{k_3} \times \frac{k_3}{k_5^{\frac{1}{2}}}$$

values of $k_3/k_5^{\frac{1}{2}}$ are obtained from the photolysis of HDAM alone, (C), and thus:

$$\frac{k_2}{k_5^{\frac{1}{2}}} = \frac{[\text{AZM-d}_6]}{[\text{substrate}]} \times \left[\frac{Rt_{CD_3H}}{Rt_{CD_4}} - \frac{Ra_{CD_3H}}{Ra_{CD_4}} \right] \times \frac{k_3}{k_5^{\frac{1}{2}}} \qquad (G)$$

Since the hexadeuteroazomethane (HDAM) used was 92% AZM-d_6 and equal partial pressures of HDAM and substrate were used, $\frac{[\text{AZM-d}_6]}{[\text{substrate}]} = 0.92$.

3.3.2. Results.

Since information on the Arrhenius parameters of deuterated azomethane is scant, the latter were fully investigated before the azomethane was photolyzed with the tetramethyl substrates.

3.3.2.1. Photolysis of Hexadeuteroazomethane alone.

Mass spectrometric analysis of the mass peaks at 19 and 20 produced the CD_3H : CD_4 and CD_3H : Total methane (CD_3H + CD_4) at each temperature. Normally, two samples were produced for each temperature and five pairs of figures for the 19 and 20 peaks obtained from the mass spectrometer for each sample. (See Table 7.)

Between two and four samples were produced for gas-liquid chromatographic analysis to obtain the rates of formation of total methane, ethane and nitrogen. (See Tables 8 and 9.)

The rates of formation thus calculated were substituted into equation (G) from section 3.3.1. to generate the rate constants $k_3/k_5^{\frac{1}{2}}$: Table 10 for azomethane-d_6 and d_5; Table 12 for (pure) azomethane-d_6. Table 11 lists the "least squares" values of $k_3/k_5^{\frac{1}{2}}$ at each temperature for the Arrhenius plot of azomethane-d_6 and d_5, (graph 4), and Table 13 the corresponding values for (pure) azomethane-d_6, (graph 5), that is, the values of $k_3/k_5^{\frac{1}{2}}$ read directly from the straight line Arrhenius plots.

The "least squares" values of $k_3/k_5^{\frac{1}{2}}$ for azomethane-d_6, listed in Table 13, were used to determine the values of $k_2/k_5^{\frac{1}{2}}$ for the Arrhenius plots of $Sn(CH_3)_4$ + HDAM and $Ge(CH_3)_4$ + HDAM by the method described in section 3.3.1..

A least squares analysis was used in every Arrhenius plot, and k_2 for hydrogen abstraction from both tetramethyl substrates was obtained using Shepp's[19] value for k_5.

Table 7. Photolysis of HDAM alone; Mass Spectrometric Analysis for Mass Peaks 19 and 20.

Temp. °C		$\frac{19}{20} = \frac{Ra_{CD_3H}}{Ra_{CD_4}}$ (average)		$\frac{Ra_{CD_3H}}{Ra_{CD_4}}$ (mean of average values)
150	(a)	0.374	}	0.371
150	(b)	0.427*		
150	(d)	0.368		
125	(a)	0.470*		
125	(b)	0.411	}	0.404
125	(c)	0.397		
100	(a)	0.406	}	0.406†
100	(b)	0.360		
75	(a)	0.489	}	0.491
75	(b)	0.493		
50	(a)	0.735	}	0.843†
50	(b)	0.843		
25	(a)	1.236	}	1.229
25	(b)	1.222		

*value ignored

†value taken as most likely after preliminary calculations

Table 8. Photolysis of HDAM alone; Gas-Liquid Chromatographic Analysis.

Temp. °C	Photolysis Time sec.	P_{HDAM} mm.	Area (in^2) Methane	Ethane	Nitrogen
150°(e)	120	30	0.34 x 32	1.28 x 32	0.89 x 256
150°(f)	120	20	0.75 x 16	3.91 x 32	0.65 x 256
125°(d)	120	20	0.36 x 32	3.72 x 64	1.70 x 128
125°(e)	120	20	0.36 x 32	6.14 x 32	1.50 x 128
100°(c)	120	20	0.18 x 16	4.95 x 32	0.74 x 128
100°(d)	120	20	0.27 x 16	4.52 x 32	1.18 x 128
100°(e)	120	20	0.49 x 8	6.11 x 32	1.60 x 128
75°(c)	120	20	0.23 x 8	4.40 x 64	0.79 x 128
75°(d)	120	20	0.69 x 4	5.15 x 64	2.00 x 64
75°(e)	120	20	0.49 x 4	3.34 x 64	0.74 x 256
50°(b)	180	20	0.64 x 4	9.60 x 64	1.55 x 128
50°(d)	120	20	0.36 x 4	3.78 x 64	1.28 x 128
50°(e)	120	20	0.24 x 4	3.35 x 64	0.73 x 256
25°(c)	120	20	0.53 x 2	4.67 x 64	1.70 x 128
25°(d)	120	20	0.09 x 2	1.58 x 32	----
25°(f)	180	20	0.07 x 4	3.18 x 32	0.50 x 128
25°(g)	120	20	0.14 x 2	6.13 x 32	1.25 x 128

Sample Calculation of rates of formation from areas of G.L.C.

(see Table 8 and Appendix 2).

Rate of formation =

$$\frac{\text{Area}}{\text{Standard Area}} \times \frac{\text{Standard Volume}}{\text{Volume of cell}} \times \frac{1}{\text{Photolysis Time}}$$

$$= \frac{\text{Area}}{\text{Standard Area}} \times \frac{1.22 \times 10^{-5}}{125.4} \times \frac{1}{120} \text{ m ml}^{-1}\text{s}^{-1}$$

At 150°C (a):

$$R_{\text{methane}} = \frac{0.34 \times 32 \times 1.122 \times 10^{-5}}{2211.58 \times 125.4 \times 120} = 3.667 \times 10^{-12} \text{ m ml}^{-1}\text{s}^{-1}$$

$$R_{\text{ethane}} = \frac{1.28 \times 32 \times 1.122 \times 10^{-5}}{3419.31 \times 125.4 \times 120} = 8.932 \times 10^{-12} \text{ m ml}^{-1}\text{s}^{-1}$$

$$R_{\text{nitrogen}} = \frac{0.89 \times 256 \times 1.122 \times 10^{-5}}{2478.4 \times 125.4 \times 120} = 6.856 \times 10^{-11} \text{ m ml}^{-1}\text{s}^{-1}$$

Table 9. Photolysis of HDAM alone; Rates of Formation of Gaseous Products.

Temp. °C	$R_{methane}$ ($m\ ml^{-1}s^{-1}$) x 10^{12}	R_{ethane} ($m\ ml^{-1}s^{-1}$) x 10^{11}	$R_{nitrogen}$ ($m\ ml^{-1}s^{-1}$) x 10^{11}	$\frac{R_{methane}}{R^{\frac{1}{2}}_{C_2D_6}}$ ($m^{\frac{1}{2}}ml^{-\frac{1}{2}}s^{-\frac{1}{2}}$) x 10^{7}	$\frac{R_{methane}}{*R^{\frac{1}{2}}_{C_2D_6}}$ ($m^{\frac{1}{2}}ml^{-\frac{1}{2}}s^{-\frac{1}{2}}$) x 10^{7}
150°(a)	3.667	0.893	6.856	12.26	12.90
150°(f)	4.046	2.729	5.006	7.745	7.83
125°(d)	3.884	5.192	6.546	5.391	5.434
125°(e)	3.884	4.285	5.776	5.933	5.981
100°(c)	0.971	3.453	2.850	1.652	1.661
100°(d)	1.456	3.154	4.544	2.592	2.614
100°(e)	1.321	4.263	6.160	2.024	2.041
75°(c)	0.6203	6.142	3.042	0.7914	0.7938
75°(d)	0.9305	7.178	3.851	1.098	1.102
75°(e)	0.6609	4.662	5.699	0.9679	0.975
50°(b)	0.5754	8.933	5.969	0.6088	0.6113
50°(d)	0.4855	5.276	4.929	0.6682	0.6720
50°(e)	0.3240	4.676	5.652	0.4734	0.4772

Table 9. Continued

25°(c)	0.3574	6.518	6.546	0.4427	0.4454
25°(d)	0.06068	1.103	1.155	0.1827	0.1840
25°(f)	0.06293	1.484	1.925	0.1633	0.1646
25°(g)	0.0944	4.278	4.813	0.1443	0.1453

$$*R^{\frac{1}{2}}_{C_2D_6} = (R_{C_2D_6} - 0.012R_{N_2})^{\frac{1}{2}}$$

Table 10. Results of the Photolysis of HDAM alone:

Rate Constants for Azomethane -d_6 and d_5 (for CD_4 only).

Temp. °C	$\frac{Ra_{methane}}{*R^{\frac{1}{2}}_{C_2D_6}}$ (†) x 10^7	$\frac{R_{CD_4}}{R_{(CD_4 + CD_3H)}}$	$\frac{Ra_{CD_4}}{*R^{\frac{1}{2}}_{C_2D_6}}$ (†) x 10^7	[Azomethane] d_6 and d_5 (m ml^{-1}) x 10^7	$\frac{k_3}{k_5^{\frac{1}{2}}}$ (‡)	log $\frac{k_3}{k_5^{\frac{1}{2}}}$	
150°(a)	12.90	$\frac{1}{1.371}$	9.409	11.38	0.8271	$\bar{1}.9176$	-0.0824
150°(f)	7.83	$\frac{1}{1.371}$	5.711	7.586	0.7527	$\bar{1}.8766$	-0.1234
125°(d)	5.434	$\frac{1}{1.404}$	3.870	8.061	0.4801	$\bar{1}.6813$	-0.3187
125°(e)	5.981	$\frac{1}{1.404}$	4.260	8.061	0.5285	$\bar{1}.7230$	-0.2770
100°(c)	1.661	$\frac{1}{1.406}$	1.181	8.602	0.1373	$\bar{1}.1377$	-0.8623
100°(d)	2.614	$\frac{1}{1.406}$	1.859	8.602	0.2162	$\bar{1}.3349$	-0.6651
100°(e)	2.041	$\frac{1}{1.406}$	1.452	8.602	0.1687	$\bar{1}.2271$	-0.7729

Table 10. Continued

75°(c)	0.7938	$\frac{1}{1.491}$	0.5324	9.217	0.05776	$\bar{2}.7617$	-1.2383
75°(d)	1.102	$\frac{1}{1.491}$	0.3791	9.217	0.08015	$\bar{2}.9039$	-1.0961
75°(e)	0.975	$\frac{1}{1.491}$	0.6539	9.217	0.07096	$\bar{2}.8510$	-1.1490
50°(b)	0.6113	$\frac{1}{1.843}$	0.3317	9.931	0.03340	$\bar{2}.5237$	-1.4763
50°(d)	0.6720	$\frac{1}{1.843}$	0.3646	9.931	0.03672	$\bar{2}.5649$	-1.4351
50°(e)	0.4772	$\frac{1}{1.843}$	0.2589	9.931	0.02607	$\bar{2}.4161$	-1.5839
25°(c)	0.4454	$\frac{1}{2.229}$	0.1986	10.76	0.01856	$\bar{2}.2686$	-1.7314
25°(d)	0.1840	$\frac{1}{2.229}$	0.08196	10.76	0.007663	$\bar{3}.8844$	-2.1156
25°(f)	0.1646	$\frac{1}{2.229}$	0.07326	10.76	0.006864	$\bar{3}.8366$	-2.1634
25°(g)	0.1453	$\frac{1}{2.229}$	0.06474	10.76	0.006057	$\bar{3}.7823$	-2.2177

* $R^{\frac{1}{2}}_{C_2D_6} = (R_{C_2D_6} - 0.012R_{N_2})^{\frac{1}{2}}$

† : units are $m^{\frac{1}{2}}ml^{-\frac{1}{2}}s^{-\frac{1}{2}}$

‡ : units are $ml^{\frac{1}{2}}m^{-\frac{1}{2}}s^{-\frac{1}{2}}$

Graph 4. Photolysis of HDAM alone: Arrhenius Parameters for D Abstraction from Azomethane-d_6 and d_5.

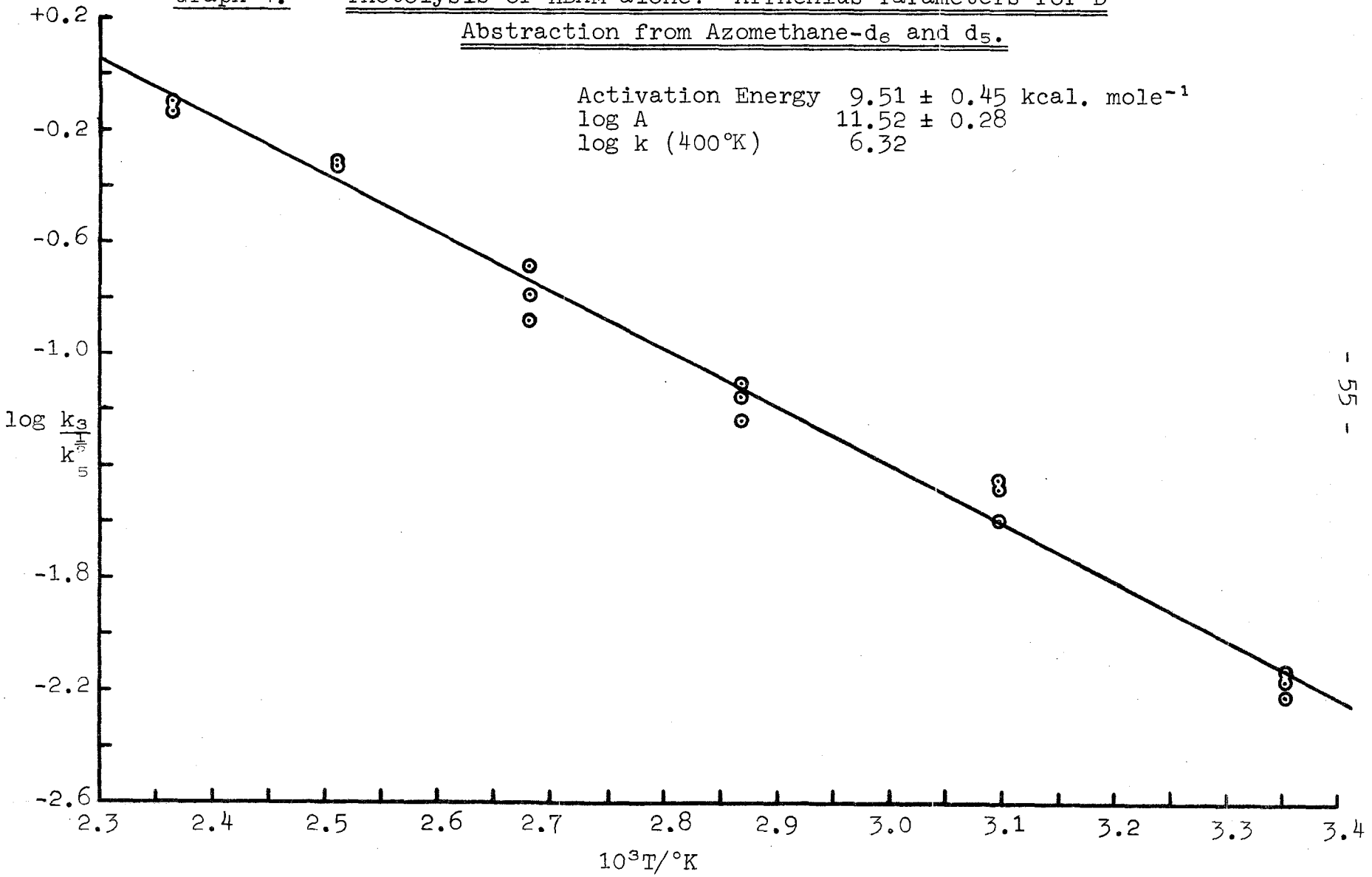

Table 11. Rate Constants for Azomethane-d_6 and d_5 from least squares Arrhenius plot (graph 4).

Temp. °C	$\log \frac{k_3}{k_5^{\frac{1}{2}}}$		$\frac{k_3}{k_5^{\frac{1}{2}}}$ $(ml^{\frac{1}{2}}m^{-\frac{1}{2}}s^{-\frac{1}{2}})$
150	-0.057	$\bar{1}.943$	0.8770
125	-0.362	$\bar{1}.638$	0.434(5)
100	-0.720	$\bar{1}.280$	0.190(5)
75	-1.118	$\bar{2}.882$	0.0762(1)
50	-1.589	$\bar{2}.411$	0.0257(6)
25	-2.123	$\bar{3}.877$	0.00753(4)

Table 12. Rate Constants for Azomethane-d_6.

Temp. °C	$\frac{Ra_{methane}}{*R^{\frac{1}{2}}_{C_2D_6}}$ (†) x 10^7	$\frac{R_{CD_4}}{R_{(CD_4 + CD_3H)}}$	$\frac{Ra_{CD_4}}{*R^{\frac{1}{2}}_{C_2D_6}}$ (†) x 10^7	[Azomethane] d_6 (m ml^{-1}) x 10^7	$\frac{k_3}{k_5^{\frac{1}{2}}}$ (‡)	log $\frac{k_3}{k_5^{\frac{1}{2}}}$	
150°(a)	12.90	$\frac{1}{1.371}$	9.409	10.47	0.8987	$\bar{1}$.9536	-0.0464
150°(f)	7.83	$\frac{1}{1.371}$	5.711	6.997	0.8162	$\bar{1}$.9118	-0.0882
125°(d)	5.434	$\frac{1}{1.404}$	3.870	7.413	0.5221	$\bar{1}$.7178	-0.2822
125°(e)	5.981	$\frac{1}{1.404}$	4.260	7.413	0.5746	$\bar{1}$.7594	-0.2406
100°(c)	1.661	$\frac{1}{1.406}$	1.181	7.911	0.1493	$\bar{1}$.1741	-0.8259
100°(d)	2.614	$\frac{1}{1.406}$	1.859	7.911	0.2350	$\bar{1}$.3711	-0.6289
100°(e)	2.041	$\frac{1}{1.406}$	1.452	7.911	0.1835	$\bar{1}$.2637	-0.7363

Table 13. Continued

75°(c)	0.7938	$\frac{1}{1.491}$	0.5324	8.477	0.06280	$\bar{2}.7980$	-1.2020
75°(d)	1.102	$\frac{1}{1.491}$	0.7391	8.477	0.08719	$\bar{2}.9404$	-1.0596
75°(e)	0.975	$\frac{1}{1.491}$	0.6539	8.477	0.07714	$\bar{2}.8873$	-1.1127
50°(b)	0.6113	$\frac{1}{1.843}$	0.3317	9.133	0.03532	$\bar{2}.5601$	-1.4399
50°(d)	0.6720	$\frac{1}{1.843}$	0.3646	9.133	0.03992	$\bar{2}.6012$	-1.3988
50°(e)	0.4772	$\frac{1}{1.843}$	0.2589	9.133	0.02835	$\bar{2}.4526$	-1.5474
25°(c)	0.4454	$\frac{1}{2.229}$	0.1986	9.896	0.02007	$\bar{2}.3025$	-1.6975
25°(d)	0.1840	$\frac{1}{2.229}$	0.08196	9.896	0.008282	$\bar{3}.9181$	-2.0819
25°(f)	0.1646	$\frac{1}{2.229}$	0.07326	9.896	0.007403	$\bar{3}.8694$	-2.1306
25°(g)	0.1453	$\frac{1}{2.229}$	0.06474	9.896	0.006542	$\bar{3}.8157$	-2.1843

$*R^{\frac{1}{2}}_{C_2D_6} = (R_{C_2D_6} + 0.012R_{N_2})^{\frac{1}{2}}$

† : units are $m^{\frac{1}{2}}ml^{-\frac{1}{2}}s^{-\frac{1}{2}}$

‡ : units are $ml^{\frac{1}{2}}m^{-\frac{1}{2}}s^{-\frac{1}{2}}$

Table 13. Rate Constants for Azomethane-d_6 from least squares Arrhenius plot (graph 5).

Temp. °C		log $\frac{k_3}{k_5^{\frac{1}{2}}}$	$\frac{k_3}{k_5^{\frac{1}{2}}}$ $(ml^{\frac{1}{2}}m^{-\frac{1}{2}}s^{-\frac{1}{2}})$
150	-0.021	$\bar{1}.979$	0.953
125	-0.326	$\bar{1}.674$	0.472
100	-0.684	$\bar{1}.316$	0.2070
75	-1.082	$\bar{2}.918$	0.0828
50	-1.553	$\bar{2}.447$	0.0280
25	-2.087	$\bar{3}.913$	0.00818(5)

Graph 5. Photolysis of HDAM alone: Arrhenius Parameters for D Abstraction from Azomethane-d_6.

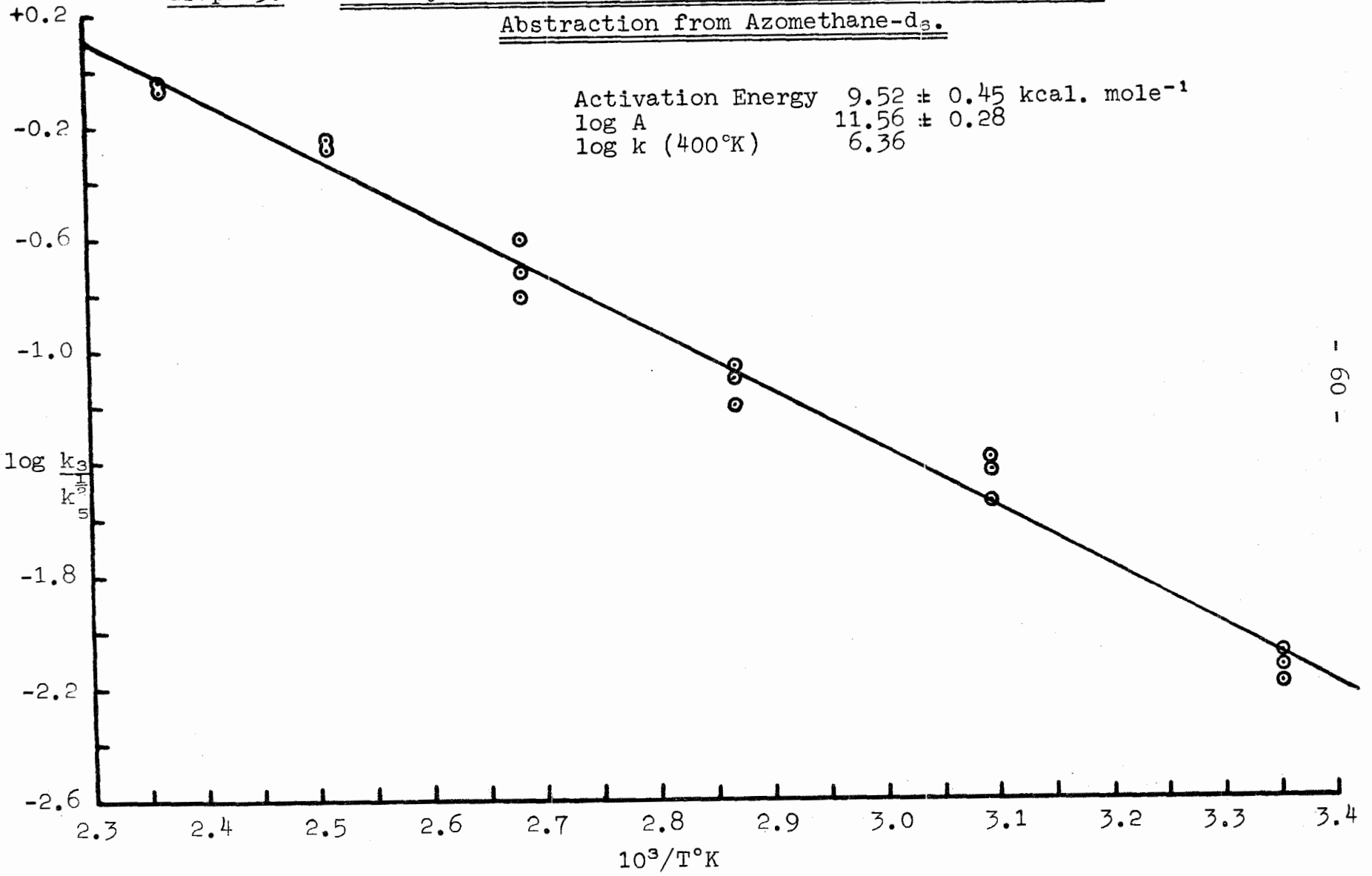

3.3.2.2. Photolysis of Hexadeuteroazomethane with Tetramethylstannane.

Mass spectrometric analysis for the mass peaks 19 and 20 were obtained at each temperature. The same procedure used for HDAM alone was followed: two samples at each temperature with five pairs of figures for the 19 and 20 peaks obtained from the mass spectrometer for each sample.

Values of $k_2/k_5^{\frac{1}{2}}$ in equation (G) in section 3.3.1. were obtained at each temperature by the method described therein, utilizing the least squares values of $k_3/k_5^{\frac{1}{2}}$, that is, those read from graph 5, the least squares Arrhenius plot for azomethane-d_6 which are listed in Table 13.

Thus the Arrhenius parameters for the abstraction of hydrogen from the substrate were evaluated from the Arrhenius plot with a least squares treatment of the raw data, and the use of Shepp's[19] value for k_5.

Table 14. Photolysis of HDAM + $Sn(CH_3)_4$; Mass Spectrometric Analysis for Mass Peaks 19 and 20.

Temp. °C	$\frac{19}{20} = \frac{Rt_{CD_3H}}{Rt_{CD_4}}$ (average)
150(a)	1.653
150(b)	1.567
125(a)	1.553
125(b)	1.512
100(a)	1.546
100(b)	1.603
75(a)	1.664
75(b)	1.776
50(a)	2.021
50(b)	1.861
25(a)	2.367
25(b)	1.927

Table 15. Results of the Photolysis of HDAM and $Sn(CH_3)_4$: Calculation of the Rate Constants.

Temp. °C		$\frac{Rt_{CD_3H}}{Rt_{CD_4}}$	$\frac{Ra_{CD_3H}}{Ra_{CD_4}}$	$\frac{R_{CD_3H}}{R_{CD_4}}$ (corrected)	$\frac{k_3}{k_5^{\frac{1}{2}}}$ ($ml^{\frac{1}{2}}m^{-\frac{1}{2}}s^{-\frac{1}{2}}$)	$\frac{k_2}{k_5^{\frac{1}{2}}}$ ($ml^{\frac{1}{2}}m^{-\frac{1}{2}}s^{-\frac{1}{2}}$)	log $\frac{k_2}{k_5^{\frac{1}{2}}}$	
150	(a)	1.653	0.371	1.282	0.9530	1.1243	0.0509	+0.0509
150	(b)	1.567	0.371	1.196	0.9530	1.0489	0.0208	+0.0208
125	(a)	1.553	0.404	1.149	0.4720	0.4992	$\bar{1}$.6983	-0.3017
125	(b)	1.512	0.404	1.108	0.4720	0.4814	$\bar{1}$.6825	-0.3175
100	(a)	1.546	0.406	1.140	0.2070	0.2172	$\bar{1}$.3369	-0.6631
100	(b)	1.603	0.406	1.197	0.2070	0.2280	$\bar{1}$.3579	-0.6421
75	(a)	1.664	0.491	1.173	0.0828	0.08939	$\bar{2}$.9513	-1.0487
75	(b)	1.776	0.491	1.285	0.0828	0.09793	$\bar{2}$.9909	-1.0091
50	(a)	2.021	0.843	1.178	0.0280	0.03034	$\bar{2}$.4820	-1.5180
50	(b)	1.861	0.843	1.018	0.0280	0.02576	$\bar{2}$.4186	-1.5814
25	(a)	2.367	1.229	1.138	0.008185	0.00857	$\bar{3}$.9332	-2.0668
25	(b)	1.927	1.229	1.698	0.008185	0.01279	2.1069	-1.8931

The average value at each temperature was used in the Arrhenius plot (graph 6).

Graph 6. Photolysis of HDAM + $Sn(CH_3)_4$: Arrhenius Parameters for H Abstraction.

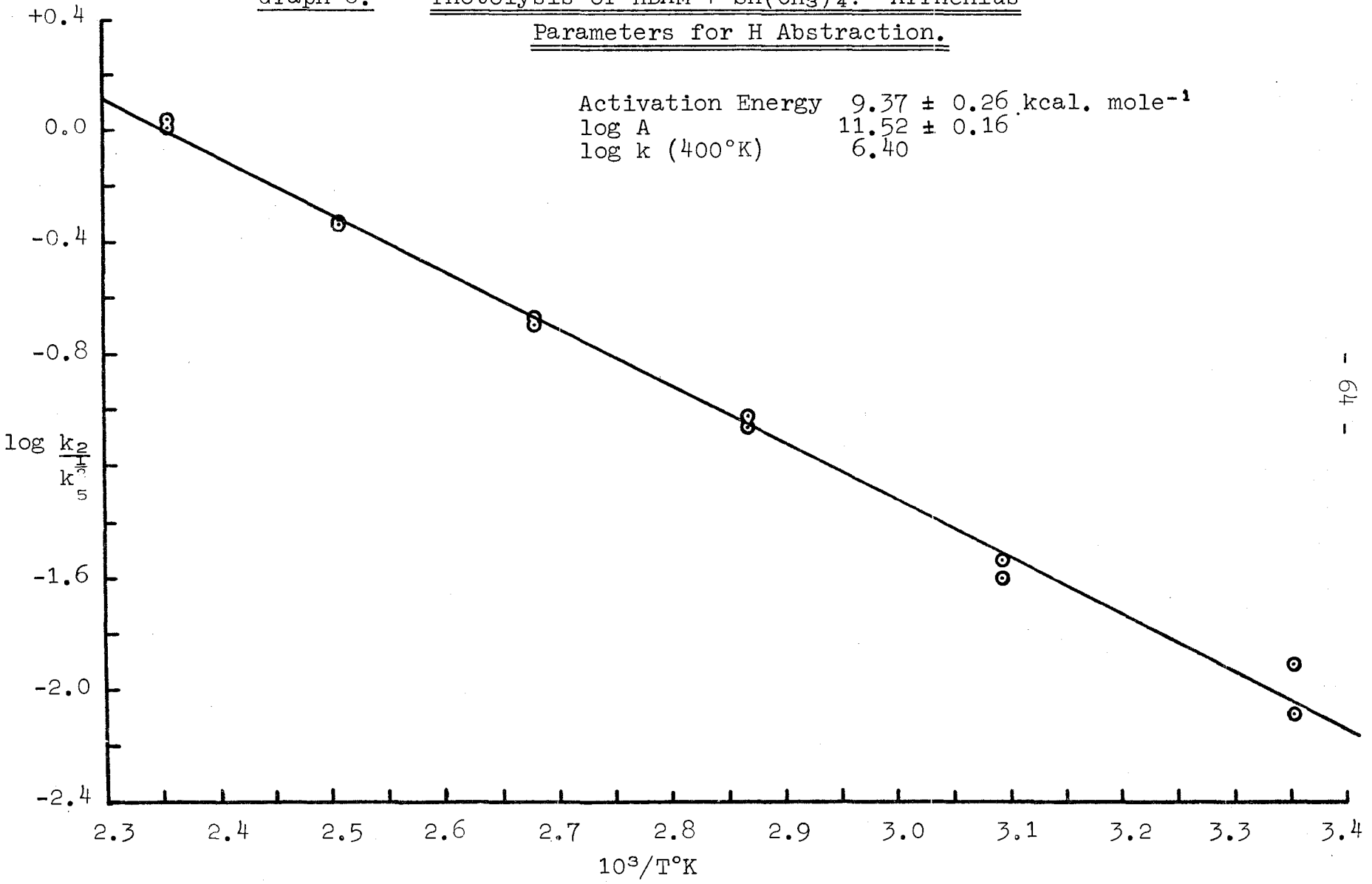

3.3.2.3. Photolysis of Hexadeuteroazomethane with Tetramethylgermane.

Mass spectrometric analysis was identical to that described in section 3.3.2.2. using $Sn(CH_3)_4$ substrate. Similarly, values of $k_2/k_5^{\frac{1}{2}}$ were obtained at each temperature using the respective values of $k_3/k_5^{\frac{1}{2}}$ read from graph 5, the Arrhenius plot for azomethane-d_6 which are listed in Table 13.

The Arrhenius parameters for the abstraction of hydrogen from the substrate were evaluated from the Arrhenius plot with a least squares treatment of the raw data, and the use of Shepp's[19] value for k_5.

Table 16. Photolysis of HDAM + $Ge(CH_3)_4$; Mass Spectrometric Analysis for Mass Peaks 19 and 20.

Temp. °C	$\frac{19}{20} = \frac{Rt_{CD_3H}}{Rt_{CD_4}}$ (average)
150(a)	1.317
150(b)	1.226
125(a)	1.457
125(b)	1.452
100(a)	1.404
100(b)	1.506
75(a)	1.823
75(b)	1.702
50(a)	2.081
50(b)	2.293
25(a)	2.974
25(b)	3.067

Table 17. Results of the Photolysis of HDAM and $Ge(CH_3)_4$: Calculation of the Rate Constants.

Temp. °C		$\frac{Rt_{CD_3H}}{Rt_{CD_4}}$	$\frac{Ra_{CD_3H}}{Ra_{CD_4}}$	$\frac{R_{CD_3H}}{R_{CD_4}}$ (corrected)	$\frac{k_3}{k_5^{\frac{1}{2}}}$ ($ml^{\frac{1}{2}}m^{-\frac{1}{2}}s^{-\frac{1}{2}}$)	$\frac{k_2}{k_5^{\frac{1}{2}}}$ ($ml^{\frac{1}{2}}m^{-\frac{1}{2}}s^{-\frac{1}{2}}$)	log $\frac{k_2}{k_5^{\frac{1}{2}}}$	
150	(a)	1.317	0.371	0.946	0.9530	0.8296	$\bar{1}$.9189	-0.0811
150	(b)	1.226	0.371	0.855	0.9530	0.7498	$\bar{1}$.8750	-0.1250
125	(a)	1.457	0.404	1.053	0.4720	0.4575	$\bar{1}$.6605	-0.3395
125	(b)	1.452	0.404	1.048	0.4720	0.4554	$\bar{1}$.0584	-0.3416
100	(a)	1.404	0.406	0.998	0.2070	0.1901	$\bar{1}$.2790	-0.7210
100	(b)	1.506	0.406	1.100	0.2070	0.2096	$\bar{1}$.3214	-0.6786
75	(a)	1.823	0.491	1.332	0.0828	0.1015	$\bar{1}$.0064	-0.9936
75	(b)	1.702	0.491	1.211	0.0828	0.09229	$\bar{2}$.9651	-1.0349
50	(a)	2.081	0.843	1.238	0.0280	0.03189	$\bar{2}$.5036	-1.4964
50	(b)	2.293	0.843	1.450	0.0280	0.03735	$\bar{2}$.5723	-1.4277
25	(a)	2.974	1.229	1.745	0.008185	0.01315	$\bar{2}$.1189	-1.8811
25	(b)	3.067	1.229	1.838	0.008185	0.01385	$\bar{2}$.1415	-1.8585

The average value at each temperature was used in the Arrhenius plot (graph 7).

Graph 7. Photolysis of HDAM + $Ge(CH_3)_4$: Arrhenius Parameters for H Abstraction.

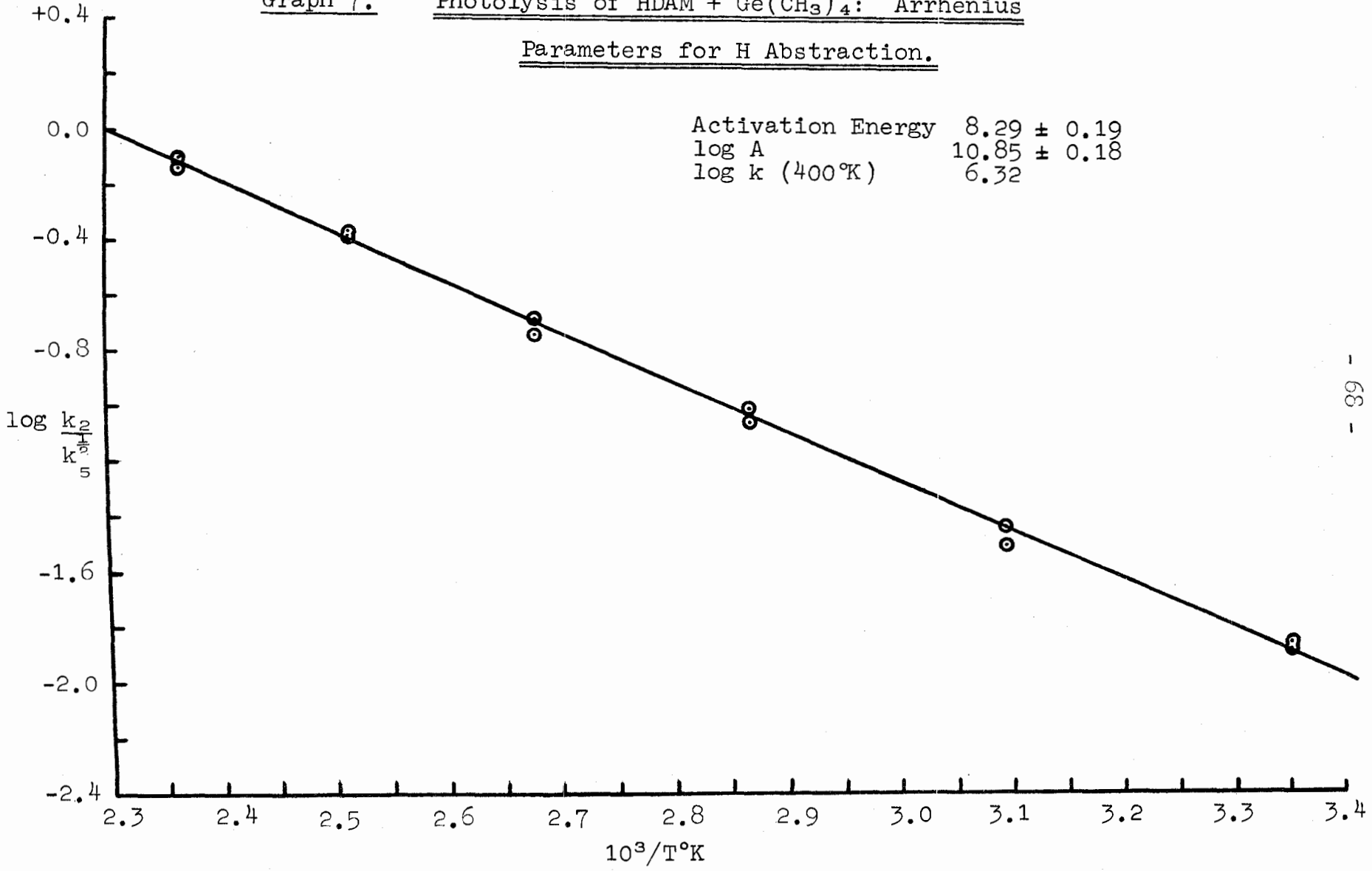

Table 18. Summary of the Arrhenius Parameters for Hydrogen Abstraction from HDAM, $Sn(CH_3)_4$ and $Ge(CH_3)_4$.

	log A	E_A (kcal mole^{-1})	$k_2 \times 10^{-6}$ at 400°K (ml m^{-1}s^{-1})	log k_2 (400°k)
$Sn(CH_3)_4$ + HDA	12.36 ± 0.21	11.65 ± 0.35	0.996	5.99
$Sn(CH_3)_4$ + HDAM	11.52 ± 0.16	9.37 ± 0.26	2.512	6.40
$Ge(CH_3)_4$ + HDA	11.46 ± 0.26	10.24 ± 0.43	0.724	5.86
$Ge(CH_3)_4$ + HDAM	10.85 ± 0.18	8.29 ± 0.19	2.089	6.32
Azomethane-d_6 and d_5 (k_D)	11.52 ± 0.28	9.51 ± 0.45	2.089	6.32
Azomethane-d_6 (k_D)	11.56 ± 0.28	9.52 ± 0.45	2.291	6.36

Table 19. Summary of Arrhenius Parameters for Hydrogen Abstraction by $\cdot CD_3$ radicals from the Group IV Tetramethyls.

HDA as radical source.

Substrate	log A	E_A (kcal mole^{-1})	$k_2 \times 10^{-6}$ (400°k) (ml m^{-1}s^{-1})	log k_2 (400°k)	log($k_2 \times 10^{-5}$) (100°C)	Proton Chemical Shift	ref.
$C(CH_3)_4$	12.30	12.00	0.549	5.74	0.2695	0.940	15
$Si(CH_3)_4$	12.00	10.79	1.288	6.11	0.6799	0.0	9
$Si(CH_3)_4$	11.84	10.36	1.585	6.20	0.7600	0.0	16
$Ge(CH_3)_4$	11.46	10.24	0.724	5.86	0.5400	0.137	*
$Sn(CH_3)_4$	12.36	11.65	0.977	5.99	0.4594	0.067	*

*this work

HDAM as radical source.

Substrate	log A	E_A (kcal mole^{-1})	$k_2 \times 10^{-6}$ (400°k) (ml m^{-1}s^{-1})	log k_2 (400°k)	log($k_2 \times 10^{-5}$) (100°C)	Proton Chemical Shift	ref.
$Ge(CH_3)_4$	10.85	8.29	2.089	6.32	1.0000	0.137	†
$Sn(CH_3)_4$	11.52	9.37	2.512	6.40	1.0302	0.067	†

†this work

Graph 8. Rate Constant (400°K) v. Proton Chemical Shift.

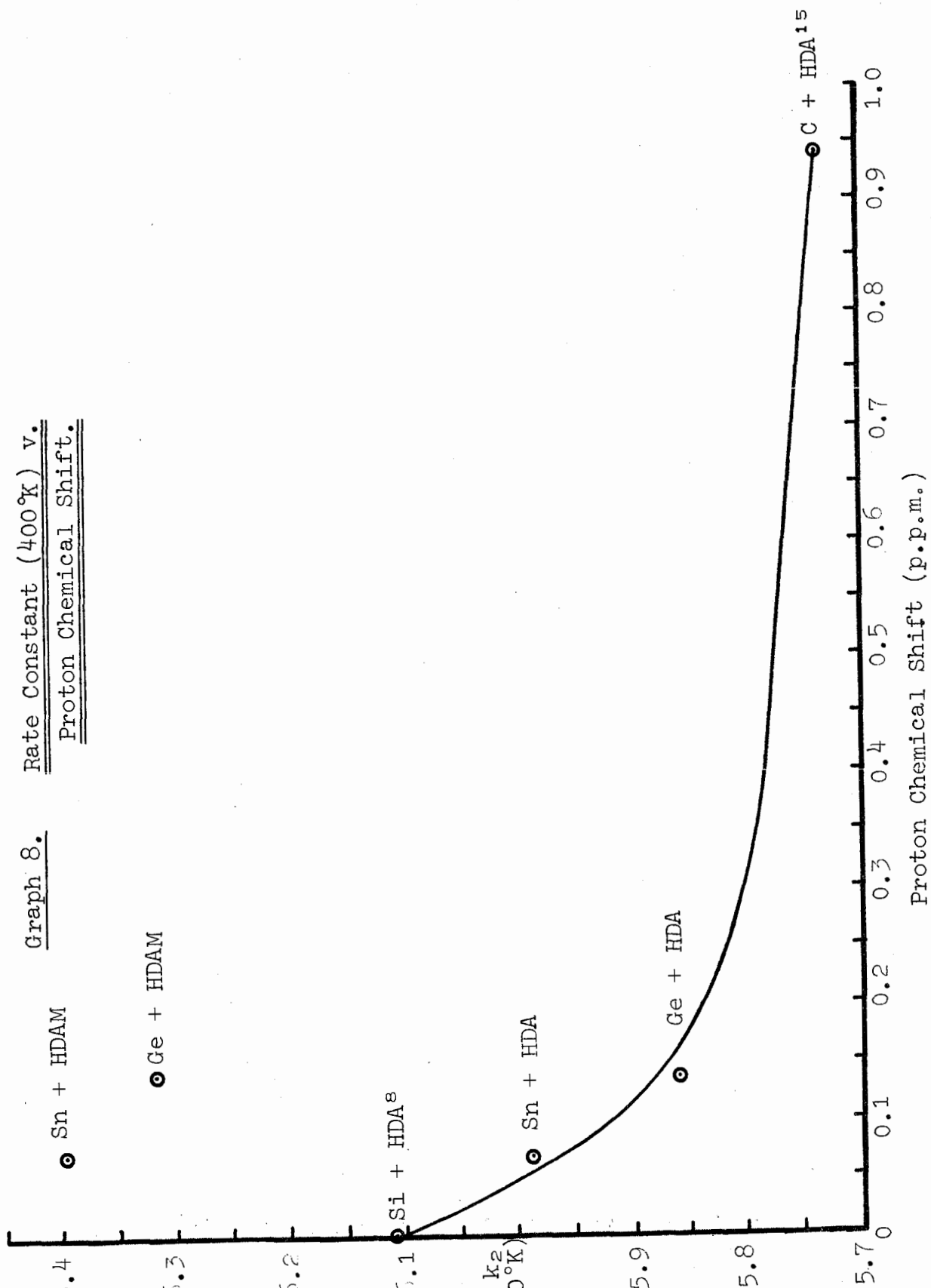

Graph 9. Rate Constant (100°C) v. Proton Chemical Shift:
A Comparison with other systems.

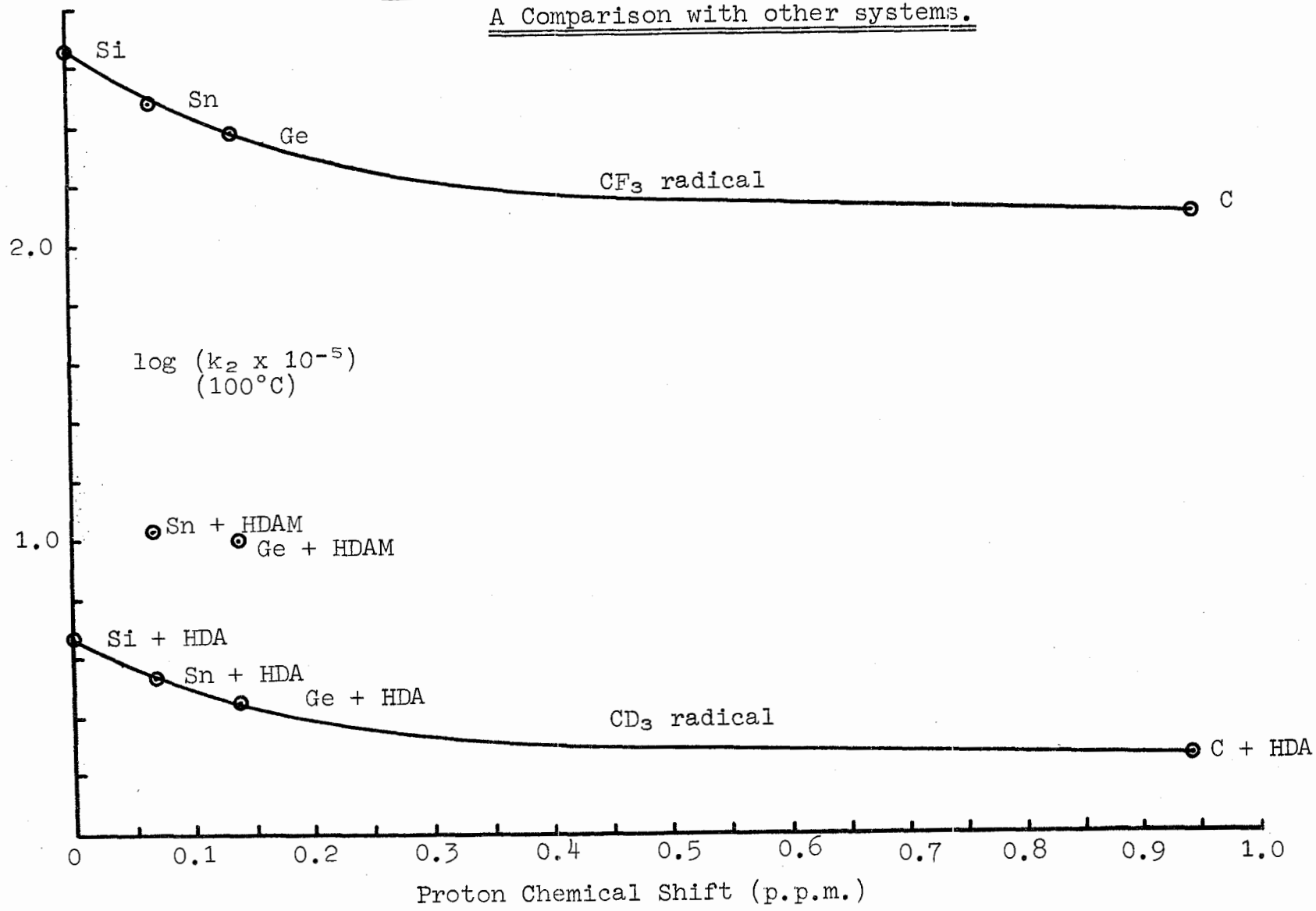

3.4. Discussion of Results for Hydrogen Abstraction.

Of the two sources of $\cdot CD_3$ radicals hexadeuteroazomethane (HDAM) was considered to be the better. In the case of hexadeuteroacetone (HDA) an additional reaction occurs at photolysis to produce acetyl ($\cdot CD_3CO$) radicals, at temperatures below about 75°C.

$$CD_3COCD_3 \xrightarrow{h\nu} \cdot CD_3 + \cdot CD_3CO \qquad 1.$$

The presence of $\cdot CD_3CO$ radicals can result in further abstraction reactions, as noted in previous work[29,39,40] and, therefore, further production of methane from equation 2.

$$\cdot CD_3 + \cdot CD_3CO \rightarrow CD_4 + \cdot CD_2CO \qquad 2.$$

$$\cdot CD_3 + CD_3COCD_3 \rightarrow CD_4 + \cdot CD_2COCD_3 \qquad 3.$$

The additional source of methane is probably the cause of upward curvature of the Arrhenius plot for the photolysis of HDA alone (see graph 1).

Since the CD_3H and CD_4 produced from the photolysis of HDA is subtracted from the total amount produced in the photolyses of HDA and the tetramethyl substrates to determine $\frac{R_{CD_3H}}{R_{CD_4}}$ (corrected) any CD_4 produced by reaction 2 is also allowed for.

However, in the presence of tetramethyl substrate, any $\cdot CD_3CO$ radicals which are not consumed in the reactions above, may well abstract hydrogen from the substrate and thereby interfere with the investigation of the abstraction by $\cdot CD_3$ radicals.

The Arrhenius plots of HDA with both $Sn(CH_3)_4$ and $Ge(CH_3)_4$ show a reasonably good straight line after a least squares evaluation but the possibility of slight curvature at both ends of the temperature range cannot be overlooked. If a least squares evaluation is performed on the points at temperatures 150-75°C in the case of $Sn(CH_3)_4$ and 150-100°C for $Ge(CH_3)_4$ (both ranges inclusive), the slope of the resultant line is steeper. A difference in activation energy of about 1.3 kcal.

mole^{-1} is noted for $Sn(CH_3)_4$ and 1.8 kcal. mole^{-1} for $Ge(CH_3)_4$. In addition, log A is increased from 12.36 to 13.08 for $Sn(CH_3)_4$ and 11.46 to 12.44 for $Ge(CH_3)_4$. This produces a value above the normal range of 11.5-12.5 in the case of $Sn(CH_3)_4$ and a value only marginally inside for $Ge(CH_3)_4$ whose value for the least squares evaluation of values at all temperatures is already rather low, just on the lower limit.

Thus although these additional plots do indicate curvature, the values found from the least squares evaluation on the points at all temperatures are preferred and are the ones reported on graphs 2 and 3 and in Tables 18 and 19.

Graph 8 shows a plot of log k_2 (400°K) v. proton chemical shift and the values of log k_2 for the $C(CH_3)_4$ + HDA[15] and $Si(CH_3)_4$ + HDA[9] systems, are added to the values obtained for $Sn(CH_3)_4$ and $Ge(CH_3)_4$ with HDA. The points approximate to a curve which shows an order of decreasing reactivity with increasing electronegativity of the central group IV atom. Graph 9 shows a similar plot of log ($k_2 \times 10^{-5}$) at 100°C v. proton chemical shift for comparison with the plot of Bell and Platt of the same group IV tetramethyls with $\cdot CF_3$ radicals. Both the plot using $\cdot CD_3$ radicals (with HDA as the radical source) and that using $\cdot CF_3$ radicals show that reactivity decreases with increasing electronegativity of the central group IV atom. The two curves are very near to being parallel; the difference between the curves is 1.97 log units at the point of $Si(CH_3)_4$, 1.84 log units at the point of $C(CH_3)_4$. The near constant difference between the two curves represents the difference in reactivity between $\cdot CF_3$ and $\cdot CD_3$ radicals.

A higher reactivity for hydrogen abstraction is shown in the $\cdot CF_3$ systems which is reflected by a higher log k_2 value, compared to the value of log k_2 with $\cdot CD_3$ and the same substrate. This demonstrates the importance of polar effects within the $\cdot CF_3$ radical; alternatively one can consider the $\cdot CF_3$ radical to be electrophilic and thus abstraction of a relatively hydridic hydrogen will be more facile.

The lack of deviation from parallelism suggests that the

polar effects, due to $\cdot CF_3$, operative in other systems, such as the methylfluorosilanes[8], are very nearly constant here for each tetramethyl. One would not expect a difference in polar effect from one tetramethyl to another because of the relatively large size and symmetry of each.

When hexadeuteroazomethane (HDAM) is used as a source of $\cdot CD_3$ radicals, there are no complications with the formation of other radicals as in the case of HDA. Two sets of Arrhenius parameters were determined in the case of azomethane alone, (Table 18), namely for deuterium abstraction from azomethane-d_6 and d_5, (graph 4) and from (pure) azomethane-d_6, (graph 5). Both plots give reasonably good straight lines and although there is a certain amount of scatter at certain temperatures there is little evidence of curvature.

The results of the latter two plots may be compared with those of other workers who have used unsubstituted azomethane ($CH_3N_2CH_3$):

	log A	E_A (kcal. mole^{-1})	log k (400°K)
Toby and Nimoy[38]	11.47	8.7 ± 0.5	6.71
Good and Thynne[41]	11.55	8.7 ± 0.2	6.79
James and Suart[34]	11.55	8.6 ± 0.5	6.85
graph 4 (AZM-d_6 and d_5)	11.52 ± 0.28	9.51 ± 0.45	6.32
graph 5 (AZM-d_6)	11.56 ± 0.28	9.52 ± 0.45	6.36

The Arrhenius parameters for deuterium abstraction show an activation energy of about 0.8 kcal. mole^{-1} higher than that noted for hydrogen abstraction; one would expect a difference[2] of about 1 kcal. mole^{-1}. All values of log A are similar thus the values of activation energy can be directly compared to show the differences in reactivity.

The values of $k_3/k_5^{\frac{1}{2}}$ from graph 5 were the ones used to evaluate $k_2/k_5^{\frac{1}{2}}$ for the tetramethyl substrates.

Graph 5 differs from graph 4 in the term concerning the

concentration of azomethane. Graph 4 is concerned with the concentration of azomethane-d_6 and d_5; graph 5 is concerned with azomethane-d_6 absolutely. This means a reduction of 8% in the concentration term since there is 8% azomethane-d_5 present. However the Arrhenius parameters are virtually unchanged.

The Arrhenius plots of the photolyses of HDAM + $Sn(CH_3)_4$, (graph 6), and of HDAM + $Ge(CH_3)_4$, (graph 7), produce very good straight lines with reproducibility of individual points at nearly every temperature. The difference between the values obtained using the average and least squares values of $k_3/k_5^{\frac{1}{2}}$ is very slight thus only those values using the latter will be discussed.

The activation energy of the HDAM + $Sn(CH_3)_4$ system is higher than that of HDAM + $Ge(CH_3)_4$, but, as in the case where HDA was used, log A for the HDAM + $Sn(CH_3)_4$ system is also higher than that of HDAM + $Ge(CH_3)_4$ which makes log k_2 for HDAM + $Sn(CH_3)_4$ higher than that for HDAM + $Ge(CH_3)_4$. This is in the same order for the substrates when used with HDA and confirms the order of reactivity with electronegativity (Chemical shift) (see Table 18 and graphs 8 and 9).

However, the log k_2 values obtained in the case where HDAM was used are higher than the corresponding values obtained with HDA as a radical source.

The difference between log k_2 (400°K) is HDAM-HDA = 6.40 - 5.99 = 0.41 for $Ge(CH_3)_4$ and 6.32 - 5.86 = 0.46 for $Sn(CH_3)_4$. Alternatively the ratios of $k_2 \times 10^{-6}$ is

$$\frac{\text{HDAM}}{\text{HDA}} = \frac{2.089}{0.724} = 2.89 \text{ for } Ge(CH_3)_4, \text{ and } \frac{2.512}{0.996} = 2.52 \text{ for } Sn(CH_3)_4.$$

It is not obvious why a difference should be caused by a change in radical source. Despite the fact that log A for HDAM + $Ge(CH_3)_4$ is outside the normal range, the Arrhenius plots obtained using HDAM as a radical source are better in that they show no signs of curvature, perhaps because HDAM is a

better source of $\cdot CD_3$ radicals; better in the sense that no complications arise due to $\cdot CD_3CO$ radicals which could compete for hydrogen abstraction.

Perhaps the uncertainty placed on the use of HDA, in the temperature range employed, manifests itself in producing incorrect values of log k_2. If the effect of $\cdot CD_3CO$ radicals is common to each tetramethyl substrate then one might still expect to see a curve representing loss of reactivity with respect to electronegativity even if it is on a qualitative basis. Such a line is seen in graph 9.

As an extension to this work it would be instructive to determine the Arrhenius parameters for the systems of HDAM with $C(CH_3)_4$, $Si(CH_3)_4$ and $Pb(CH_3)_4$ to see whether a plot of log k_2 v. chemical shift for the group IV tetramethyls with HDAM as a radical source, would also give a line similar to that obtained with HDA, only with higher log k_2 values for each substrate.

3.5. Secondary Reactions - Radical Exchange.

3.5.1. Kinetics.

Of the secondary reactions described in the past literature, hot molecule formation followed by β-fluoro rearrangement and olefin elimination, is noted for $\cdot CF_3$ radicals only. A β-deutero rearrangement is not expected on energetic grounds and only radical exchange has been investigated.

It is proposed that exchange occurs between $\cdot CD_3$ radicals and CH_3 groups from the tetramethyl substrate. This necessitates that the group IV element Sn or Ge utilizes its empty d orbitals to attain a 5 co-ordinate intermediate:
Radical exchange:

$$\cdot CD_3 + M(CH_3)_4 \rightleftarrows [CD_3 - M(CH_3)_4] \rightarrow CD_3M(CH_3)_3 + \cdot CH_3 \qquad 1.$$

Previous work[18,30] has shown the importance of empty orbitals on the central metal atom; exchange is absent in the case of neopentane where the carbon atom has no vacant orbitals of a compatible energy.

Thus $\cdot CH_3$ radicals are present as well as $\cdot CD_3$ and $\cdot CD_2H$ species and the following processes are possible:
Abstraction:

$$\cdot CD_3 + M(CH_3)_4 \rightarrow CD_3H + \cdot CH_2M(CH_3)_3 \qquad 2.$$
$$\cdot CD_2H + M(CH_3)_4 \rightarrow CD_2H_2 + \cdot CH_2M(CH_3)_3 \qquad 3.$$
$$\cdot CH_3 + M(CH_3)_4 \rightarrow CH_4 + \cdot CH_2M(CH_3)_3 \qquad 4.$$

Recombination:

$$\cdot CD_3 + \cdot CD_3 \rightarrow C_2D_6 \qquad 5.$$
$$\cdot CD_3 + \cdot CD_2H \rightarrow C_2D_5H \qquad 6.$$
$$\cdot CD_3 + \cdot CH_3 \rightarrow CD_3CH_3 \qquad 7.$$
$$\cdot CD_2H + \cdot CD_2H \rightarrow C_2D_4H_2 \qquad 8.$$
$$\cdot CD_2H + \cdot CH_3 \rightarrow C_2D_2H_4 \qquad 9.$$
$$\cdot CH_3 + \cdot CH_3 \rightarrow C_2H_6 \qquad 10.$$

Experimentally, only the products of equations 2, 5, 6 and 7 were obtained in measurable amounts.

3.5.2. Results with Hexadeuteroacetone.

3.5.2.1. Hexadeuteroacetone and Tetramethylstannane, (Table 20).

Temps. °C	Factor	Mass Peaks (in.) 30	31	32	33	34	35	36
150(a)	x200	10.90	1.6	47.38	1.25	8.3	0.6	12.85
150(b)	x200	10.05	1.75	45.38	1.2	7.75	0.6	12.5
125(a)	x200	10.05	1.6	35.9	1.2	7.6	0.6	12.0
100(a)	x200	10.65	1.35	48.75	1.2	8.4	0.6	13.2
75(a)	x200	12.2	1.8	53.75	1.35	8.95	0.7	14.45
50(a)	x200	13.15	1.7	57.5	1.6	10.15	0.7	15.55
25(a)	x200	5.95	1.55	24.63	0.7	4.2	0.25	6.6

Each set of figures was analyzed as follows: the contribution to the various peaks due to C_2D_6 was subtracted, this contribution being indicated by the 36 peak. Pro rata contributions to the 34, 32 and 30 peaks were calculated using the table in appendix 5. A small contribution of C_2D_5H, indicated by a small 35 peak was treated in a similar fashion. In every case the 34 peak was exhausted after allowing for C_2D_5H, thus no $C_2D_4H_2$ was noted. CD_3CH_3 was indicated by a residue of 33 peak.

Sample Calculations

150°(a)

	30	31	32	33	34	35	36
	10.90	1.6	47.38	1.25	8.3	0.6	12.85
C_2D_6 :	12.75		60.0		9.45		12.85
remainder	0.	1.6	0.	1.25	0.	0.6	0.
C_2D_5H:	0.38	1.32	1.19	0.33	0.11	0.6	
remainder	0.	0.28	0.	0.92	0.	0.	
CD_3CH_3:	3.1	0.66	0.45	0.92			
	0.	0.	0.	0.			

thus

C_2D_6	:	C_2D_5H	:	CD_3CH_3
12.85	:	0.6	:	0.92
21.40	:	1.0	:	1.53

150°(b)

	30	31	32	33	34	35	36
	10.05	1.75	45.38	1.2	7.75	0.6	12.5
C_2D_6 :	12.4		58.56		9.2		12.5
remainder	0.	1.75	0.	1.2	0.	0.6	0.
C_2D_5H :	0.38	1.32	1.19	0.33	0.11	0.6	
remainder	0.	0.43	0.	0.87	0.	0.	
CD_3CH_3:	2.94	0.62	0.43	0.87			
	0.	0.	0.	0.			

thus

C_2D_6	:	C_2D_5H	:	CD_3CH_3
12.5	:	0.6	:	0.87
20.83	:	1.0	:	1.45

Table 21. HDA + $Sn(CH_3)_4$: Radical Exchange.

Temp. °C	C_2D_6 :	C_2D_5H :	CD_3CH_3 or C_2D_6 :	CD_3CH_3
150(a)	21.4 :	1.0 :	1.53	14.0 : 1.0
150(b)	20.8 :	1.0 :	1.45	14.4 : 1.0
125(a)	20.0 :	1.0 :	1.45	13.8 : 1.0
100(a)	22.0 :	1.0 :	1.45	15.2 : 1.0
75(a)	20.6 :	1.0 :	1.38	15.0 : 1.0
50(a)	22.2 :	1.0 :	1.73	12.8 : 1.0
25(a)	26.4 :	1.0 :	2.25	11.7 : 1.0

3.5.2.2. Hexadeuteroacetone with Tetramethylgermane, (Table 22).

Temp. °C		Factor	Mass Peaks (in.) 30	31	32	33	34	35	36
150	(a)	x200	20.1	2.5	83.0	2.2	13.4	1.1	20.8
150	(b)	x100	14.6	2.0	65.0	1.65	11.05	0.8	16.6
137.5	(a)	x100	12.65	1.6	55.0	1.4	8.9	0.6	13.5
125	(a)	x100	14.15	1.85	66.5	1.5	10.4	0.7	16.0
125	(b)	x100	15.85	1.95	68.25	1.75	11.65	0.8	17.6
100	(a)	x100	19.6	2.5	88.0	2.2	14.9	1.0	22.4
75	(a)	x100	22.3	2.85	99.5	2.6	16.25	1.3	24.85
75	(b)	x100	15.3	2.2	68.0	1.7	11.6	0.7	17.2
50	(a)	x 50	20.9	2.75	93.4	2.35	15.3	1.2	23.35
50	(b)	x100	12.55	1.5	50.5	1.3	9.05	0.6	13.85
25	(a)	x 50	15.55	2.05	69.0	1.6	10.8	0.82	16.25
25	(b)	x100	5.95	0.7	25.2	0.5	4.1	0.25	6.6

Each set of figures was analyzed in exactly the same way as those involving $Sn(CH_3)_4$ with HDA. Analysis produced the following results in Table 23 overleaf.

Table 23. HDA + $Ge(CH_3)_4$: Radical Exchange.

Temp. °C		C_2D_6 :	C_2D_5H :	CD_3CH_3 or C_2D_6 :	CD_3CH_3
150	(a)	18.9 :	1.0 :	1.45	13.1 : 1.0
150	(b)	20.75 :	1.0 :	1.51	13.7 : 1.0
137.5	(a)	22.5 :	1.0 :	1.45	15.5 : 1.0
125	(a)	22.85 :	1.0 :	1.59	14.4 : 1.0
125	(b)	22.0 :	1.0 :	1.64	13.5 : 1.0
100	(a)	22.4 :	1.0 :	1.65	13.6 : 1.0
75	(a)	19.15 :	1.0 :	1.45	13.2 : 1.0
75	(b)	24.6 :	1.0 :	1.88	13.1 : 1.0
50	(a)	19.4 :	1.0 :	1.40	13.9 : 1.0
50	(b)	19.75 :	1.0 :	1.61	12.3 : 1.0
25	(a)	19.8 :	1.0 :	1.40	14.1 : 1.0
25	(b)	26.4 :	1.0 :	1.45	18.2 : 1.0

3.5.2.3. Discussion of Results.

Common to both $Sn(CH_3)_4$ and $Ge(CH_3)_4$ is the fact that only the ethanes C_2D_6, C_2D_5H and CD_3CH_3 are found by the analysis described in sections 3.5.2.1. and 3.5.2.2.. Subtraction of the contributions[42] due to C_2D_6 and C_2D_5H, in every case, completely accounts for the 34 peak, thus $C_2D_4H_2$ is not present in measurable quantities. Similarly, the contributions due to CD_3CH_3, (based on the remainder of the 33 peak), erase that remaining of peaks 33, 32, 31 and 30. The absence of any contribution of mass 30 suggests that there is not a measurable amount of C_2H_6.

Therefore, it was impossible to determine the cross-combination ratio, Φ, in the manner of previous work[18,30].

from equations 5, 7, 10: $$\Phi = \frac{R_{CD_3CH_3}}{R_{C_2H_6}^{\frac{1}{2}} \; R_{C_2D_6}^{\frac{1}{2}}}$$

If Φ is assumed to be unity, $R_{C_2H_6}$ would be less than 0.01 times smaller than $R_{CD_3CH_3}$. This is too small to be detected under the conditions employed.

A similar argument explains the fact that no $C_2D_4H_2$ was detected; the $\cdot CD_2H$ radicals are present in small quantity since the HDA contains only 5% CD_2HCOCD_3.

Nor is it possible to set up a material balance relationship where the concentration of carbon monoxide is related to the addition of all methanes and ethanes because of lack of sufficient information.

Since the subtraction of pro rata contributions produces negative answers to the peaks at 34, 32, 31 and 30 it was felt unjustified to make a fully quantitative critique of the ratios of C_2D_6 : C_2D_5H : CD_3CH_3.

However, a qualitative assessment of the ratios of the ethanes, (Tables 21 and 23), shows that they are fairly constant and independent of temperature. Certainly there is no obvious trend and one can only conclude that under the experimental conditions employed these statements hold. In this

case one may deduce that the ratio of C_2D_6 : CD_3CH_3 is about 14 : 1 for both $Sn(CH_3)_4$ and $Ge(CH_3)_4$.

Alternatively, the amount of radical exchange can be expressed as a percentage, deduced from the experimental findings. For example, in the case of $Sn(CH_3)_4$, and assuming that the presence of each $\cdot CH_3$ radical means the previous presence of a $\cdot CD_3$ radical which has been lost by exchange:

$$C_2D_6 : C_2D_5H : CD_3CH_3$$
$$21.2 : 1.0 : 1.5 \quad \text{(in the average case)}$$

$$\therefore CD_3 : CH_3 \text{ is } (42.4 + 1.0 + 3.0) : 1.5$$
$$100 : 3.4$$

Thus about 3.5% of the $\cdot CD_3$ radicals are lost by exchange with $Sn(CH_3)_4$ to produce $\cdot CH_3$ radicals, assuming that the $\cdot CD_2H$ radicals are present in small enough quantities that they do not add significantly to the exchange process.

A figure of 3.5% is obtained for the HDA + $Ge(CH_3)_4$ system also.

3.5.3. Results with Hexadeuteroazomethane.

3.5.3.1. Hexadeuteroazomethane and Tetramethylstannane, (Table 24).

Temp. °C	Factor	Mass Peaks (in.) 30	31	32	33	34	35	36
150(a)	x 50	25.4	1.9	95.0	2.15	15.5	0.55	21.5
125(a)	x 50	31.0	2.0	118.0	2.5	19.1	0.8	26.0
125(b)	x 50	29.2	2.45	113.32	2.4	17.9	0.7	25.0
100(a)	x100	23.8	1.9	91.0	1.7	14.4	0.6	20.2
75(a)	x100	25.6	1.7	96.0	1.8	14.3	0.675	21.7
50(a)	x100	28.9	2.1	121.5	2.4	19.4	0.75	13.65
25(a)	x100	27.3	2.35	110.5	2.0	16.2	0.65	22.9

These figures were analyzed by the procedure described in section 3.4.2.1. for HDA and $Sn(CH_3)_4$. The 36, 35 and 33 peaks were taken as indicating C_2D_6, C_2D_5H and CD_3CH_3 respectively and pro-rata contributions were subtracted from the whole range (30 - 36) using appendix 3. Analysis produced the following results in Table 25 overleaf.

Table 25. HDAM + $Sn(CH_3)_4$: Radical Exchange.

Temp. °C	C_2D_6	C_2D_5H	CD_3CH_3 or C_2D_6	CD_3CH_3
150(a)	39.1 :	1.0 :	3.36	11.65 : 1.0
125(a)	32.5 :	1.0 :	2.58	12.40 : 1.0
125(b)	35.7 :	1.0 :	2.88	12.62 : 1.0
100(a)	33.7 :	1.0 :	2.28	14.77 : 1.0
75(a)	32.2 :	1.0 :	2.12	15.19 : 1.0
50(a)	36.4 :	1.0 :	2.65	13.74 : 1.0
25(a)	35.2 :	1.0 :	2.53	13.95 : 1.0

3.5.3.2. Hexadeuteroazomethane and Tetramethylgermane, (Table 26).

Temp. °C	Factor	Mass Peaks (in.) 30	31	32	33	34	35	36
150(b)	x100	14.0	1.2	56.5	1.08	9.0	0.32	12.4
125(a)	x100	20.5	1.55	83.0	1.75	13.15	0.6	18.0
100(b)	x100	18.9	1.35	76.0	1.6	12.6	0.575	17.8
75(a)	x100	28.0	1.85	116.0	2.5	18.5	0.8	26.1
50(b)	x100	11.6	0.8	46.68	0.9	7.3	0.2	10.1
25(b)	x200	11.8	0.75	48.0	0.98	7.9	0.3	10.8

Once again, analysis was effected using the method described in section 3.4.2.1. with the values listed in appendix 5 for the contributions for the isotopic species of ethane involved in this system. Thus the following results were obtained in Table 27 overleaf.

Table 27. HDAM + $Ge(CH_3)_4$: Radical Exchange.

Temp. °C	C_2D_6 :	C_2D_5H :	CD_3CH_3 or C_2D_6 :	CD_3CH_3
150(b)	38.8 :	1.0 :	2.82 13.73 :	1.0
125(a)	30.0 :	1.0 :	2.36 12.70 :	1.0
100(b)	31.0 :	1.0 :	2.23 13.88 :	1.0
75(a)	32.6 :	1.0 :	2.57 12.68 :	1.0
50(b)	40.4 :	1.0 :	3.05 13.25 :	1.0
25(b)	36.0 :	1.0 :	2.71 13.27 :	1.0

3.5.3.3. Discussion of Results.

In essence the discussion here parallels that concerning radical exchange with HDA (Section 3.5.2.3), the intrinsic difference being that HDAM has a larger amount of isotopic impurity.

With both $Sn(CH_3)_4$ and $Ge(CH_3)_4$ substrates, the only ethanes present in an amount detectable by mass spectrometric evaluation were C_2D_6, C_2D_5H and CD_3CH_3. Even though the azomethane was found to contain 8% $CD_2HN_2CD_3$ impurity, neither $C_2D_4H_2$ nor C_2H_6 could be measured because subtraction of pro-rata contributions in connexion with peaks of higher mass produced left negative amounts for the 34 and 30 peaks.

Thus once again, the cross-combination ratios concerning CD_3CH_3 and C_2D_5H could not be determined. If Φ is assumed to be unity then, respectively, ${}^{R}C_2H_6$ and ${}^{R}C_2D_4H_2$ would be less than 0.01 times smaller than ${}^{R}C_2D_6$. Both are too small to be detected under the conditions employed.

A material balance equation relating the concentration of nitrogen to the addition of methanes and ethanes was not considered because of lack of sufficient information.

As with the HDA systems, a full quantitative appraisal is deemed unjustified but qualitatively similar deductions can be made concerning the independence from temperature of the ethane ratios (and thus the amount of radical exchange).

The ratio of C_2D_6 : CD_3CH_3 is about 13.5 : 1 for $Sn(CH_3)_4$ and about 13 : 1 for $Ge(CH_3)_4$ which compares reasonably well with the figures obtained with the HDA systems.

It is noted that there is less C_2D_5H produced in the HDAM systems compared with HDA which is surprising since there is a larger isotopic impurity present in HDAM.

Nevertheless, the "percentage of radical exchange" for both substrates is very close to that with HDA. The same assumptions are made; namely, that each $\cdot CH_3$ radical present represents the previous loss of a $\cdot CD_3$ radical by exchange, and

the $\cdot CD_2H$ radicals do not exchange too.

Thus, for $Ge(CH_3)_4$:

C_2D_6 : C_2D_5H : CD_3CH_3

34.8 : 1.0 : 2.62 (in the average case)

$\therefore CD_3 : CH_3$ is $(69.6 + 1.0 + 5.24) : 2.62$

$75.84 : 2.62$

$100 : 3.5$

This suggests that about 3.5% of the $\cdot CD_3$ radicals exchange with $Ge(CH_3)_4$ to produce $\cdot CH_3$ radicals, which figure is also obtained for the HDAM + $Sn(CH_3)_4$ system.

Thus both tetramethyl substrates show the same amount of radical exchange with both radical sources using this rudimentary approach.

However, more work of a more quantitative nature is required to completely investigate the several possibilities of reactions.

Appendix 1. Comparison of the Arrhenius Parameters of some Silanes with their Carbon analogues; references 2,43,44,45.

	log A	E_A (kcal. mole^{-1})
$^{\cdot}CH_3 + C^{14}H_4 \rightarrow CH_4$	11.83	14.65
$^{\cdot}CD_3 + C^{14}D_4 \rightarrow CD_4$	12.60	17.80
$^{\cdot}CD_3 + C_2H_6 \rightarrow CD_3H$	12.21	11.8
$^{\cdot}CD_3 + C_2D_6 \rightarrow CD_4$	12.21	13.3
$^{\cdot}CH_3 + SiH_4 \rightarrow CH_4$	11.80 ± 0.32	6.99 ± 0.56
$^{\cdot}CH_3 + SiD_4 \rightarrow CH_3D$	11.98 ± 0.37	8.19 ± 0.65
$^{\cdot}CH_3 + Si_2H_6 \rightarrow CH_4$	11.96 ± 0.18	5.63 ± 0.32
$^{\cdot}CH_3 + Si_2D_6 \rightarrow CH_3D$	12.19 ± 0.21	6.96 ± 0.35

Appendix 2. Standard Areas of Selected Gases for Gas-Liquid Chromatographic Analysis.

Standard conditions:

Chart speed	: 2 in min^{-1}
Detector current	: 9 milliamps.
Column	: Porapak Q
Column temperature	: 0°C
Flushing gas	: Helium
Flushing speed	: 50 ml min^{-1}
Standard volume	: 1.122×10^{-5} moles.

Standard areas:

CH_4	: 2211.6 in^2
C_2H_6	: 3419.3 in^2
C_2F_6	: 5331.6 in^2
N_2	: 2478.4 in^2

Appendix 3. Relationship of concentration to partial pressure of reactant in reaction cell (volume = 125.4 ml) for the temperature range 25 - 150°C.

Temp.	Partial Pressure (mm)	Conc. (m ml^{-1}) x 10^7	$\log_{10}$ Conc.	
150°C (423.16°K)	30	11.38	$\bar{6}.0561$	-5.9439
	20	7.586	$\bar{7}.8800$	-6.1200
125°C (398.16°K)	30	12.09	$\bar{6}.0825$	-5.9175
	20	8.061	$\bar{7}.9064$	-6.0936
100°C (373.16°K)	30	12.91	$\bar{6}.1109$	-5.8891
	20	8.602	$\bar{7}.9346$	-6.0654
75°C (348.16°K)	30	13.82	$\bar{6}.1406$	-5.8594
	20	9.217	$\bar{7}.9646$	-6.0354
50°C (323.16°K)	30	14.89	$\bar{6}.1729$	-5.8271
	20	9.931	$\bar{7}.9970$	-6.0030
25°C (298.16°K)	30	16.44	$\bar{6}.2159$	-5.7841
	20	10.76	6.0320	-6.9680

Appendix 4. Fortran IV Computer Programme for Least-Squares Evaluation.

Cards as printed:

```
C       LEAST SQUARES EVALUATION
C       A=INTERCEPT, B=SLOPE, C=ST. DEV. OF A, D=ST. DEV. OF B
C       E=ST. DEV. OF ENTIRE FIT(PLATT), F=ACTIVATION ENERGY
C       G=ST. DEV. OF ENTIRE FIT(SLADE)
        DIMENSION T(50),Y(50),TITLE(19),X(50)
9       READ(5,100,END=8)N,TITLE
100     FORMAT(I3,19A4)
        WRITE(6,200)TITLE
200     FORMAT('1',19A4////)
        READ(5,101) (T(I),Y(I),I=1,N)
101     FORMAT(2F10.0)
C       CALCULATE RECIPROCAL TEMPERATURES
        DO 99 I=1,N
99      X(I)=1.0/(T(I)+273.16)
        CALL PWSLS(X,Y,A,B,C,D,E,F,G,N,RLOGA,RLOGK,RLOGW,
      $RLOGZ,CHISQ)
        WRITE(6,202)B,D,F,A,C,RLOGA,RLOGK,RLOGW,RLOGZ,E,G,CHISQ
202     FORMAT('  SLOPE = ',G15.5,5X,'       STANDARD
      $DEVIATION = ',G15.5,//'  ACTIVATION ENERGY = ',G15.5///
      $'  INTERCEPT = ',G15.5,5X,'      STANDARD
      $DEVIATION = ',G15.5///'  LOG A = ',G15.5//
      $'  LOG K AT 400 K = ',G15.5,5X,
      $'  LOG K AT 1/T=0.0023 = ',G15.5,
      $'  LOG K AT 1/T=0.0033 = ',G15.5///
      $' PLATT ERROR IN ENTIRE FIT =',G15.5///
      $' SLADE ERROR IN ENTIRE FIT =',G15.5///
      $' CHISQ =',G15.5/////)
        WRITE(6,203)
203     FORMAT(4X,' TEMP',4X,'YEXPT',5X,'YCALC',6X,'DIFF'///)
        DO 98 I=1,N
        YCALC=A+B*X(I)
        DIFF=Y(I)-YCALC
98      WRITE(6,204)T(I),Y(I),YCALC,DIFF
204     FORMAT(F10.1,3F10.5)
        GO TO 9
8       STOP
        END
```

Appendix 4. Continued

```
      SUBROUTINE PWSLS(X,Y,A,B,C,D,E,F,G,N,RLOGA,RLOGK,RLOGW,
     £RLOGZ,CHISQ)
C     PETER SLADE'S OWN LEAST SQUARES PROGRAMME TO FIT
     £Y=A+B*X
      DIMENSION X(50),Y(50)
      SX=0.0
      SY=0.0
      SXY=0.0
      SX2=0.0
      DO 89 I=1,N
      SX=SX+X(I)
      SY=SY+Y(I)
      SXY=SXY+X(I)*Y(I)
89    SX2=SX2+X(I)*X(I)
      Z=N*SX2-SX*SX
      A=(SX2*SY-SX*SXY)/Z
      B=(N*SXY-SX*SY)/Z
      YMEAN=SY/N
      R=0.0
      SIG=0.0
      DO 88 I=1,N
      YCALC=A+B*X(I)
      SIG=SIG+(Y(I)-YMEAN)**2
88    R=R+(YCALC-Y(I))**2
      SIGMA=SIG/N
      S=SQRT(R/(N-3.0))
      C=SQRT(SX2/Z)*S
      D=SQRT(N/Z)*S
      E=SQRT(R/(N-1.0))
      F=B*(-4.5738)
      G=SQRT(R/Z)*S
      CHISQ=R/(SIGMA)*(SIGMA)
      RLOGA=A+6.67
      RLOGK=RLOGA+B*0.0025
      RLOGW=A+B*0.0023
      RLOGZ=A+B*0.0033
      RETURN
      END
```

Appendix 5. Mass Spectra Data; reference 42.

For an ionization voltage of 70 volts:

$\frac{m}{e}$	CD_3 | CD_3	CD_3 | CD_2H	CD_2H | CD_2H	CD_3 | CH_3	CDH_2 | CDH_2	CDH_2 | CH_3	CH_3 | CH_3
36	100						
35		100					
34	73.6	18.7	100				
33		55.2	36.5	100			
32	468.8	197.5	117.4	49.2	100		
31		220.0	230.4	71.6	64.2	100	
30	99.2	63.6	156.5	337.4	258.1	72.9	100

Bibliography.

1. F. A. Cotton and G. Wilkinson, "Advanced Inorganic Chemistry," 456, John Wiley and Sons, New York, (1967).

2. O. P. Strausz, E. Jakubowski, H. S. Sandhu, H. E. Gunning, J. Chem. Phys., 51, 552 (1969).

3. D. P. Craig, A. Maccoll, R. S. Nyholm, L. E. Orgel and L. E. Sutton, J. Chem. Soc. A, 332 (1954).

4. B. J. Aylett, Advances in Inorg. Chem. and Radiochem., 11, 249 (1968).

5. J. A. Kerr, D. H. Slater and J. C. Young, J. Chem. Soc. A, 104 (1956).

6. T. N. Bell and B. B. Johnson, Austral. J. Chem., 20, 1545 (1967).

7. J. A. Kerr, A. Stephens and J. C. Young, Int. J. Chem. Kin., 1, 371 (1969).

8. T. N. Bell and U. F. Zucker, J. Phys. Chem., 74, 979 (1969).

9. T. N. Bell and A. E. Platt, ibid., 75, 603 (1971).

10. T. N. Bell and U. F. Zucker, Can. J. Chem. 48, 1209 (1970).

11. W. J. Cheng and M. Szwarc, J. Phys. Chem., 72, 494 (1968).

12. T. N. Bell and A. E. Platt, Int. J. Chem. Kin., 2, 299 (1970).

13. A. U. Chaudhry and B. G. Gowenlock, J. Organomet. Chem., 16, 221 (1969).

14. E. R. Morris and J. C. J. Thynne, ibid., 17, 3 (1969).

15. J. A. Kerr, D. Timlin, J. Chem. Soc. A, 1241 (1969).

16. J. A. Kerr, A. Stephens and J. C. Young, Int. J. Chem. Kin., 1, 339 (1969).

17. T. N. Bell and U. F. Zucker, Can. J. Chem., 47, 1701 (1969).

Bibliography. Continued

18. T. N. Bell and A. E. Platt, Chem. Comm., 325 (1970).

19. A. Shepp, J. Chem. Phys., 24, 939 (1956).

20. R. E. March and J. C. Polanyi, Proc. Royal Soc. A, 273, 360 (1963)..

21. P. B. Ayscough, J. Chem. Phys., 24, 944 (1956).

22. A. F. Trotman-Dickenson, Chemistry and Industry, 379 (1965).

23. E. A. V. Ebsworth and J. J. Turner, J. Phys. Chem., 67, 805 (1963).

24. E. A. V. Ebsworth and S. G. Frankiss, Trans. Farad. Soc., 59, 1518 (1963).

25. W. McFarlane, Molecular Physics, 13, 587 (1967).

26. A. F. Trotman-Dickenson, J. R. Birchard and E. W. R. Steacie, J. Chem. Phys., 19, 163 (1951).

27. G. O. Pritchard, H. O. Pritchard, H. I. Schiff, A. F. Trotman-Dickenson, Trans. Farad. Soc., 52, 849 (1956).

28. R. E. Rebbert and P. Ausloos, J. Amer. Chem. Soc., 86, 2068 (1964).

29. R. D. Giles and E. Whittle, Trans. Farad. Soc., 61, 1425 (1965).

30. T. N. Bell and A. E. Platt, To be published.

31. J. C. Calvert and J. N. Pitts, "Photochemistry," 732, John Wiley and Sons, New York, (1966).

32. W. J. Cheng, J. Nimoy and S. Toby, J. Phys. Chem., 71, 3075 (1967).

33. Sir H. Melville and B. G. Gowenlock, "Experimental Methods In Gas Reactions," 242, MacMillan, London, (1964).

34. D. G. L. James and R. D. Suart, Trans. Farad. Soc. 63, 2708 (1967).

35. M. H. Jones and E. W. R. Steacie, J. Chem. Phys., 21, 1018 (1953).

Bibliography. Continued

36. R. E. Berkley, Private communication.

37. R. F. Hutton and C. Steel, J. Amer. Chem. Soc., 86, 745 (1964).

38. S. Toby and J. Nimoy, J. Phys. Chem., 70, 867 (1966).

39. H. Shaw and S. Toby, ibid., 72, 2337 (1968).

40. P. Ausloos and E. W. R. Steacie, Can. J. Chem., 33, 47 (1955).

41. A. Good and J. C. J. Thynne, Trans. Farad. Soc., 63, 2708 (1967).

42. Y. Amenomiya and R. F. Pottie, Can. J. Chem., 46, 1735 (1968).

43. F. S. Dainton, K. J. Ivin and F. Wilkinson, Trans. Farad. Soc., 55, 929 (1959).

44. F. S. Dainton, E. A. Creak and K. J. Ivin, ibid., 58, 326 (1962).

45. F. E. Saalfeld and H. J. Svec, J. Phys. Chem., 70, 1753 (1966).